

1 **Significant inter-annual fluctuation in CO₂ and CH₄ diffusive**
2 **fluxes from subtropical aquaculture ponds: Implications for**
3 **climate change and carbon emission evaluations**

4 Ping Yang^{a,b,c,d*}, Linhai Zhang^{a,b,c}, Yongxin Lin^{a,b,c}, Hong Yang^{e,f}, Derrick
5 Y. F. Lai^g, Chuan Tong^{a,b,d*}, Yifei Zhang^a, Lishan Tan^e, Guanghui Zhao^a,
6 Kam W. Tang^{h*}

7 ^a*School of Geographical Sciences, Fujian Normal University, Fuzhou 350007, P.R.*
8 *China,*

9 ^b*Key Laboratory of Humid Subtropical Eco-geographical Process of Ministry of*
10 *Education, Fujian Normal University, Fuzhou 350007, P.R. China*

11 ^c*Fujian Provincial Key Laboratory for Subtropical Resources and Environment, Fujian*
12 *Normal University, Fuzhou 350117, P.R. China*

13 ^d*Research Centre of Wetlands in Subtropical Region, Fujian Normal University, Fuzhou*
14 *350007, P.R. China*

15 ^e*Department of Geography and Environmental Science, University of Reading, Reading,*
16 *UK*

17 ^f*College of Environmental Science and Engineering, Fujian Normal University, Fuzhou*
18 *350007, China*

19 ^g*Department of Geography and Resource Management, The Chinese University of*
20 *Hong Kong, Shatin, New Territories, Hong Kong SAR, China*

21 ^h*Department of Biosciences, Swansea University, Swansea SA2 8PP, U. K.*

22 ***Corresponding author:**

23 *E-mail address:* yangping528@sina.cn (P. Yang); tongch@fjnu.edu.cn (C. Tong); Kam
24 W. Tang (k.w.tang@swansea.ac.uk)

25 **Telephone:** 086-0591-87445659 **Fax :** 086-0591-83465397

26 **ABSTRACT**

27 Aquaculture ponds are potential hotspots for carbon cycling and emission of greenhouse
28 gases (GHGs) like CO₂ and CH₄, but they are often poorly assessed in the global GHG
29 budget. This study determined the temporal variations of CO₂ and CH₄ concentrations and
30 diffusive fluxes and their environmental drivers in coastal aquaculture ponds in
31 southeastern China over a five-year period (2017–2021). The findings indicated that CH₄
32 flux from aquaculture ponds fluctuated markedly year-to-year, and CO₂ flux varied
33 between positive and negative between years. The coefficient of inter-annual variation of
34 CO₂ and CH₄ diffusive fluxes was 168% and 127%, respectively, highlighting the
35 importance of long-term observations to improve GHG assessment from aquaculture
36 ponds. In addition to chlorophyll-*a* and dissolved oxygen as the common environmental
37 drivers, CO₂ was further regulated by total dissolved phosphorus and CH₄ by dissolved
38 organic carbon. Feed conversion ratio correlated positively with both CO₂ and CH₄
39 concentrations and fluxes, showing that unconsumed feeds fueled microbial GHG
40 production. A linear regression based on binned (averaged) monthly CO₂ diffusive flux
41 data, calculated from CO₂ concentrations, can be used to estimate CH₄ diffusive flux with
42 a fair degree of confidence ($r^2 = 0.66$; $p < 0.001$). This algorithm provides a simple and
43 practical way to assess the total carbon diffusive flux from aquaculture ponds. Overall,
44 this study provides new insights into mitigating the carbon footprint of aquaculture
45 production and assessing the impact of aquaculture ponds on the regional and global
46 scales.

47 *Keywords:* Greenhouse gases; Diffusive flux; Carbon footprint; Climate impact;

49 **1. Introduction**

50 Methane (CH₄) and carbon dioxide (CO₂) are the two primary greenhouse gases
51 (GHGs), together contributing over 80% of the total atmospheric radiative forcing
52 (Friedlingstein et al., 2022; Le Quéré et al., 2018; Myhre et al., 2013). In 2023, the
53 atmospheric CO₂ and CH₄ concentrations have reached 420 ppm and 1900 ppb,
54 respectively (National Oceanic and Atmospheric Administration, 2023), which is
55 approximately 48% and 156% over the pre-industrial values. To mitigate global carbon
56 emission, China has pledged to cap its carbon emission by 2030 and achieve net-zero
57 emission by 2060 (Yang et al., 2022a). However, identifying the sources and quantifying
58 the magnitude of GHG emissions are crucial for predicting and reducing GHG emissions
59 (Borges et al., 2015; Jia et al., 2022; Yang et al., 2023a).

60 Carbon emissions from inland aquatic ecosystems such as lakes, rivers and reservoirs
61 have been quite well studied (Bastviken et al., 2011; Raymond et al., 2013; Wang et al.,
62 2019), but emissions from small and shallow ponds (<0.001km²) are still poorly
63 quantified and are often excluded from the global GHG budget (Holgerson, 2015;
64 Holgerson and Raymond, 2016). There are estimated 3.2 billion small ponds globally
65 (Downing, 2010), covering a total area of ~0.8 million km² (Holgerson and Raymond,
66 2016). Due to their relatively high organic loading (Rubbo et al., 2006), these ponds can
67 be hotspots for carbon cycling (Holgerson, 2015) and GHG emissions (e.g., Jensen et al.,
68 2023; Peacock et al., 2021; Prėskienis et al., 2021). Among the small ponds, aquaculture
69 ponds are of particular interest thanks to the fast-growing aquaculture sector world-wide

70 (Naylor et al., 2021). In aquaculture ponds, the persistent introduction of fertilizers,
71 animal wastes and feeds can significantly elevate the production and release of GHGs, a
72 phenomenon not often observed in natural ponds (Boyd et al., 2010; Chanda et al., 2019;
73 Tong et al., 2020).

74 Approximately 25,700 km² in China is occupied by aquaculture ponds (Chen et al.,
75 2015, 2016), and about 60% of them are concentrated in estuaries and coastal bays (Duan
76 et al., 2020). Most of them are small-hold aquaculture farms that are subject to
77 fluctuations in ambient conditions (e.g., air temperature, sunlight, precipitation) and
78 different farming practices (Chen et al., 2016; Kosten et al., 2020; Yang et al., 2023b),
79 leading to considerable variations in GHG production and emissions from the ponds (e.g.,
80 Dong et al., 2023a; Liu et al., 2016; Zhao et al., 2021). As the two major carbon-based
81 GHGs, the dynamics of CO₂ and CH₄ are controlled by different organisms and biological
82 processes: CO₂ is consumed by photoautotrophs via photosynthesis and produced by
83 heterotrophs via respiration (Gudas et al., 2010; Liu et al., 2010), whereas
84 methanogenesis is largely driven by methanogens in the anoxic sediment (Lin and Lin,
85 2022; Segers, 1998; Gruca-Rokosz et al., 2020), with some contribution from the
86 water-column (Bogard, et al., 2014; Tang et al., 2016). On the other hand, the two gases
87 are connected within the carbon cycle, e.g., organic carbon can feed into both respiration
88 and methanogenesis; CH₄ and CO₂ can also be interconverted by methanotrophs and
89 methanogens, respectively, under specific conditions (Chowdhury and Dick, 2013;
90 Zabranska and Pokorna, 2018). Therefore, we may expect some empirical relationships
91 between the two gases in aquaculture ponds.

92 Due to logistical limitations, researchers usually make measurements at low
93 frequency (once a month or less) and for a short duration (no more than two years). This
94 may not be sufficient to reveal the temporal variations in GHG emissions. Given the sheer
95 number of small-hold aquaculture ponds in China, it is impractical for officials to monitor
96 them all. Proper assessment of GHG emissions may therefore require self-monitoring and
97 reporting by the farmers, but the farmers usually lack the time, skills or equipment to do
98 rigorous gas measurements. Between the two gases, CO₂ can be measured relatively
99 easily using inexpensive sensors (e.g., [Zosel et al., 2011](#)). By developing simple
100 algorithms to estimate CH₄ from CO₂ data, we can greatly expand the nation's ability to
101 assess the combined carbon emission from the fast-growing aquaculture sector.

102 In this study, we measured the concentrations of dissolved CO₂ and CH₄ in the water
103 column of aquaculture ponds in southeastern China over five years between 2017–2021,
104 from which we calculated the diffusive flux of CO₂ and CH₄ across the air-water interface.
105 The objectives were to determine the magnitude and temporal variations of CO₂ and CH₄
106 concentrations and diffusive fluxes and the key environmental drivers. We then examined
107 the empirical relationships between CO₂ and CH₄ by binning the data at different
108 temporal resolutions, in order to derive useful algorithms for assessing GHG outputs from
109 aquaculture ponds.

110

111 **2. Materials and methods**

112 *2.1. Study areas*

113 Measurements and sample collections took place in the Shanyutan Wetland, located
114 within the Min River estuary in the Fujian province, China (26°00'36"–26°03'42"N,
115 119°34'12"–119°41'40"E, [Figure 1](#)). The region is characterized by a subtropical marine
116 monsoon climate typical of the southern regions, with an average yearly temperature of
117 19.6 °C and an annual precipitation of approximately 1,350 mm ([Yang et al., 2020a](#)). In
118 this region, the prevalent plant species include the indigenous *Phragmites australis* and
119 *Cyperus malaccensis*, along with the non-native *Spartina alterniflora* ([Gao et al., 2019](#);
120 [Tong et al., 2018](#)). Over the past decades, extensive areas of the tidal saltmarshes have
121 been transformed into aquaculture shrimp ponds. The aquacultural production period is
122 typically from May to November, with one crop of shrimp (*Litopenaeus vannamei*)
123 produced per year. Previous research provides comprehensive information on the
124 aquaculture ponds and associated farming techniques ([Tong et al., 2020](#)).

125 2.2. Collection of water samples

126 Three shrimp ponds were sampled 1–3 times each month between 2017 and 2021. In
127 each pond, water samples from 20-cm depth were collected using an organic glass
128 hydrophores at three different sites ([Tian et al., 2023](#); [Yang et al., 2020b](#)). Subsequently,
129 the water was poured into 150-mL polyethylene bottles and into 55-mL pre-weighed
130 serum glass bottles. Before the bottles were sealed, a 0.2 mL saturated HgCl₂ solution was
131 added to halt microbial processes ([Borges et al., 2018](#); [Marescaux et al., 2018](#)). A total of
132 648 water samples were obtained and promptly transported to the laboratory in ice coolers
133 within 4-6 h.

134 2.3. Measurement of dissolved gas concentrations

135 The levels of dissolved CO₂ (C_{CO_2}) and CH₄ (C_{CH_4}) in the water samples were
136 measured with the headspace equilibration method (Yang et al., 2019; Zhang et al., 2021).
137 Briefly, water samples without bubble were gathered in 55 mL serum glass bottles that
138 had been pre-weighed. In the laboratory, a headspace was formed by injecting 25 mL of
139 ultrahigh purity nitrogen (N₂) gas (99.999%) into each glass bottle. Afterwards, the bottles
140 were vigorously shaken in an oscillator (IS-RDD3, China) for 10 min to attain
141 equilibrium between the atmospheric and water phases (Cotovicz Jr et al., 2016).
142 Following a 30-minute settling period, a 5-ml sample of the headspace was extracted and
143 injected into a Shimazu GC-2010 gas chromatograph (Kyoto, Japan) equipped with a
144 flame ionization detector (FID) to measure CO₂ and CH₄. Five standards CO₂ (or CH₄)
145 gas, namely 50 (2), 100 (8), 500 (500), 3000 (1000) and 10,000 (10,000) ppm, were used
146 to calibrate the FID.. Using the specific water and headspace volumes in the glass bottles,
147 along with the solubility coefficient of CO₂ (or CH₄) for the specific temperature and
148 salinity, the *in situ* C_{CO_2} (or C_{CH_4} ; $\mu\text{mol L}^{-1}$) was calculated (Wanninkhof, 1992).

149 2.4. Calculations of diffusive GHG fluxes

150 Diffusive fluxes of CO₂ (F_{CO_2} ; $\text{mmol m}^{-2} \text{h}^{-1}$) and CH₄ (F_{CH_4} ; $\mu\text{mol m}^{-2} \text{h}^{-1}$) across
151 the air-water interface were determined based on Equation 1 (Cotovicz Jr et al., 2016; Jia
152 et al., 2022; Musenze et al., 2014):

$$153 \quad F_{\text{gas}} = k_x \times (C_w - C_{\text{eq}}) \quad (1)$$

154 where F_{gas} was the diffusive flux of CO₂ (or CH₄); C_w was the concentrations of dissolved
155 CO₂ (or CH₄) ($\mu\text{mol L}^{-1}$) in the surface water; C_{eq} was the concentration of CO₂ (or CH₄)
156 ($\mu\text{mol L}^{-1}$) at equilibrium with the overlying atmosphere at the *in situ* conditions. The

157 coefficient for gas exchange k_x (cm h⁻¹) was calculated as (Crusius and Wanninkhof,
158 2003):

$$159 \quad k_x = [2.07 + (0.215 \times U_{10}^{1.7})] \times \left(\frac{Sc_{\text{gas}}}{600}\right)^{-n} \quad (2)$$

160 where $U_{10}^{1.7}$ was the wind speed without friction (m s⁻¹) measured at a height of 10 m
161 above the aquatic surface (Crusius and Wanninkhof, 2003); n was the proportionality
162 coefficient, which depended on $U_{10}^{1.7}$ (if $U_{10}^{1.7} > 3$ m s⁻¹, then $n = 1/2$; if $U_{10}^{1.7} \leq 3$ m s⁻¹,
163 then $n = 2/3$) (Cole and Caraco, 1998). Sc_{gas} was the Schmidt number of CO₂ (or CH₄)
164 calculated from Eq. (3) and Eq. (4);

$$165 \quad Sc_{\text{CO}_2} = 2073.1 - 125.62t + 3.6276t^2 - 0.043219t^3 \quad (3)$$

$$165 \quad Sc_{\text{CH}_4} = 2039.2 - 120.31t + 3.4209t^2 - 0.040437t^3 \quad (4)$$

166 where t was the surface water temperature (°C).

167 The calculated CH₄ flux was converted to CO₂-equivalent flux based on the
168 conversion factor of 45 for a 100-year time horizon (Neubauer and Megonigal, 2019), and
169 added to the calculated CO₂ emission to determine the total CO₂-equivalent emission.

170 2.5. Ancillary environmental variables

171 During each sampling campaign, *in situ* measurements were taken at a water depth
172 of 20 cm at each location. These measurements included water temperature (T_w), pH,
173 salinity and dissolved oxygen (DO) using a portable pH/Temperature meter (IQ150, USA),
174 a Eutech Instruments-Salt6 salinity meter (USA) and a 550A YSI multiparameter probe
175 (Yellow Springs, OH, USA). The MRE weather station provided data on meteorological
176 variables, such as air temperature (T_A), wind speed (W_S) and air pressure (A_P), measured
177 with the Vantage Pro 2 automatic meteorological station (Hayward, CA, USA).

178 In the laboratory, we filtered the water samples through 0.45- μ m acetate fiber
179 membranes. Subsequently, we measured the filtrates for their content of dissolved organic
180 carbon (DOC) with a TOC-VCPH/CPN Analyzer (Shimadzu, Japan), and total dissolved
181 phosphorus (TDP) and total dissolved nitrogen (TDN) with a flow injection analyzer
182 (Skalar Analytical SAN⁺⁺, Netherlands). Chlorophyll-*a* (Chl-*a*) was extracted in 90%
183 ethanol (or acetone) in darkness for 24 h and then measured on a Shimadzu UV-2450
184 UV–visible spectrophotometer (Kyoto, Japan) (Kang et al., 2023; Xu et al., 2017). Feed
185 conversion ratio of the farmed organisms was determined by dividing the total dry feed
186 weight provide by the overall weight increase (Zhang et al., 2018).

187 *2.6. Statistical analysis*

188 Before conducting statistical tests, we assessed the data for normal distribution. The
189 coefficient of variation for CO₂ (or CH₄) fluxes were determined by dividing the standard
190 deviation by the average value. The effect of sampling years on environmental factors,
191 concentrations of dissolved GHGs, and diffusive fluxes was evaluated using a one-way
192 ANOVA in IBM's SPSS 22.0 software (Armonk, NY, USA). To assess the relationships
193 between environmental factors and dissolved GHG concentrations or diffusive fluxes, we
194 employed the Spearman correlation method, using the vegan package in R Version 4.1.0
195 (R Foundation for Statistical Computing, 2013), and redundancy analysis (RDA) using
196 the software CANOCO version 5.0 (Microcomputer Power, Ithaca, NY, USA). Partial
197 least square structural equation modeling (PLS-SEM) was conducted in R Version 4.1.0
198 (R Foundation for Statistical Computing, 2013) with the ‘semPLS’ package to evaluate
199 the direct or indirect effect of environmental variables on the GHGs. More details of the

200 PLS-SEM analysis can be found in [Tan et al. \(2022, 2023\)](#).

201 To derive predictive relationship between CO₂ concentration (or diffusive fluxes) and
202 CH₄ concentration (or diffusive fluxes), we ran linear regressions through the data at
203 different resolutions: raw data without binning; binning (averaging) data by months, by
204 seasons and by year. We compared the regression outputs and considered an r^2 value of $>$
205 0.5 to be suitable for applications. For all statistical analyses, a significance threshold of p
206 < 0.05 was used.

207

208 **3. Results**

209 *3.1. Physico-chemical properties and feed conversion ratio*

210 The physico-chemical properties of the pond's surface water are shown in [Figure 2](#).
211 There were significant between-year differences in all of the variables. T_w averaged
212 $\sim 28^\circ\text{C}$ in 2017-2018, but was significantly lower in 2019-2021 ([Figure 2a](#)). Salinity was
213 at 3.5 ‰ in the first two years, then increased significantly in 2019 and again in 2020
214 ([Figure 2b](#)). Water pH was between 8.75 and 9.25, except in 2019 when it dropped to 7.5
215 ([Figure 2c](#)). Mean DO was $> 6 \text{ mg L}^{-1}$ with higher concentrations in 2018 and 2020
216 ([Figure 2d](#)).

217 DOC ranged from 10.6 to 17.7 mg L^{-1} , with a significantly higher concentration in
218 2017 ([Figure 2e](#)). TDN varied between 1.2 and 2.0 mg L^{-1} , and was significantly higher in
219 2019 ([Figure 2f](#)). TDP and Chl-*a* exhibited similar temporal variations over the five-year
220 period: lowest in 2017 and highest in 2020 ([Figures 2g,h](#)).

221 Feed conversion ratio varied significantly over time, with the highest value of 1.9 in
222 2017, followed by 1.5 in 2019, 1.3 in 2020, 1.1 in 2021, and 0.7 in 2018 (Figure S1).

223 3.2. Inter-annual variations in GHG concentrations and fluxes

224 C_{CO_2} and F_{CO_2} varied significantly between years ($p < 0.001$; Figure 3). The highest
225 annual mean C_{CO_2} was $37.4 \pm 2.6 \mu\text{mol L}^{-1}$ in 2017, and the lowest at $10.9 \pm 0.9 \mu\text{mol L}^{-1}$
226 in 2017 (Figure 3a). F_{CO_2} ranged from $-0.12 \pm 0.03 \text{ mmol m}^{-2} \text{ h}^{-1}$ in 2020 to 1.3 ± 0.2
227 $\text{mmol m}^{-2} \text{ h}^{-1}$ in 2017 (Figure 3b). C_{CH_4} varied significantly between $0.48 \pm 0.06 \mu\text{mol L}^{-1}$
228 and $4.3 \pm 0.8 \mu\text{mol L}^{-1}$ across the years ($p < 0.001$; Figure 3c). F_{CH_4} also varied
229 significantly with time, between 15.0 to $153.7 \mu\text{mol m}^{-2} \text{ h}^{-1}$ ($p < 0.001$; Figure 3d).

230 The combined CO_2 -eq diffusive flux showed significant variations over time (Figure
231 4), and the coefficient of variation was 133.9%. Over the five-year period, the mean
232 combined diffusive flux ranged from 28.9 ± 5.3 to $695.9 \pm 152.4 \text{ kg CO}_2\text{-eq ha}^{-1} \text{ yr}^{-1}$
233 (Figure 4), with an average value of $206.8 \pm 123.9 \text{ kg CO}_2\text{-eq ha}^{-1} \text{ yr}^{-1}$. CH_4 accounted for
234 over 70% of the combined CO_2 -eq diffusive flux in each year.

235 3.3. Environmental drivers of GHG concentrations and diffusive fluxes

236 According to Spearman correlations (Figure S2) and RDA analysis (Figure 5), the
237 inter-annual variations in C_{CO_2} and F_{CO_2} were strongly driven by Chl-*a*, DO and TDP,
238 which together explained 79.5% of the variations. The inter-annual variations in C_{CH_4} and
239 F_{CH_4} were primarily determined by DOC, Chl-*a* and DO, which together explained 93.7%
240 of the variations.

241 Based on PLS-SEM analysis, Chl-*a*, DO and TDP all had a direct negative effect on
242 C_{CO_2} , which in turn affected F_{CO_2} (Figure 6a). DO also had a direct negative effect on

243 F_{CO_2} . TDP positively influenced Chl-*a*, which in turn had a positive effect on DO. C_{CH_4}
244 was affected positively by DOC and negatively by Chl-*a* and DO; these then indirectly
245 affected F_{CH_4} (Figure 6b). Salinity had a negative effect on DOC and F_{CH_4} .

246 3.4. Predictive relationships between CO_2 and CH_4

247 We ran linear regressions using CO_2 concentration (or flux) as the independent
248 variable and CH_4 concentration (or flux) as the predicted variable. We started with raw
249 data without binning, then gradually decreased the resolution by binning (average) the
250 data by month, season or year (Figure 7). With raw data, the relationship was not
251 significant for concentration, but it was significant for flux despite the very low r^2 value
252 (Table 1). By binning the data, the regressions were all significant and the r^2 value
253 increased. The r^2 value for concentration data was lower than 0.5 in all but the lowest
254 resolution (yearly average), whereas the r^2 value for flux data was at 0.66 or higher (Table
255 1).

256

257 4. Discussion

258 4.1. Effects of feed conversion ratio

259 In aquaculture, feeds are applied to sustain the animals (Avnimelech and Ritvo, 2003;
260 Chen et al., 2016; Pouil et al., 2019), but only a small fraction of these feeds is effectively
261 transformed into biomass (Flickinger et al., 2020; Molnar et al., 2013; Sahu et al., 2013).
262 The efficiency at which the animals utilize the feeds is expressed as feed conversion ratio
263 (FCR = amount of feed/amount of biomass produced). In this study, we found that FCR

264 varied significantly between years (Figure S1), which may be a result of variable survival
265 and physiological state of the farmed animals, or quality of the feeds. FCR correlated
266 positively with DOC and negatively with DO (Figure 8), suggesting that unconsumed
267 feeds were decomposed into dissolved organics that subsequently fueled microbial
268 respiration, as supported by the positive correlations between FCR and C_{CO_2} and F_{CO_2}
269 (Figures 9a and 9b). Unconsumed feeds and other organic wastes could also accelerate
270 methane production, as shown by the positive correlations of FCR with C_{CH_4} and F_{CH_4}
271 (Figures 9c and 9d).

272 4.2. Environmental drivers of CO_2

273 The surface-water CO_2 concentration exhibited remarkable variations across the
274 five-year period and the aquaculture ponds switched between being a source and a sink of
275 CO_2 to the atmosphere (Figures 3a and 3b). CO_2 was consumed via photosynthesis by
276 microalgae, as indicated by the significant negative correlation between Chl-*a* and C_{CO_2}
277 and F_{CO_2} (Figure S2a). Microalgal biomass in the aquaculture ponds was regulated by
278 dissolved nutrients such as TDP but not TDN (Figure S2a). This may be attributed to the
279 high TDN (1.2~2.0 mg L⁻¹; Figure 2f) and low TDP (0.1~0.3 mg L⁻¹; Figure 2g)
280 concentrations resulting in a strong P-limitation (Bernhard and Peele, 1997; Lapointe et
281 al., 2015). The key role of TDP in regulating CO_2 was also confirmed by PLS-SEM
282 analysis (Figure 6a).

283 Our correlation (Figure S2a) and RDA (Figure 5a) analyses showed that water
284 temperature (T_w) was an important driver of C_{CO_2} and F_{CO_2} . The inter-annual variability
285 in T_w in the ponds was approximately 5 °C, with considerably lower values in 2017 and

286 2018. Not only that higher water temperature would increase the system respiration and
287 DOC mineralization, but it may also decrease photosynthetic CO₂ uptake by negatively
288 impacting Chl-*a* (Figure S2a). Together, this would increase CO₂ concentration and flux
289 (Gudasz et al., 2010; Xiao et al., 2020; Huttunen et al., 2003).

290 4.3. Environmental drivers of CH₄

291 The average concentrations of dissolved CH₄ in the ponds was 800–8,000%
292 saturated relative to the atmosphere, making the ponds a net source of CH₄ to the air
293 (Figure 3), similar to others inland aquatic ecosystems (Borges et al., 2015; Natchimuthu
294 et al., 2016; Praetzel et al., 2021). The very high C_{CH₄} in the aquaculture ponds could be
295 attributed to the high DOC loading (Figure 5b), likely from unconsumed feeds and animal
296 wastes (Figure 8; Yang et al., 2020b), which fueled CH₄ production (Berberich et al., 2020;
297 Davidson et al., 2018; Zhou et al., 2018). This was further supported by the significant
298 correlation found (1) between feed conversion rate and DOC concentrations ($p < 0.001$;
299 Figure 8c), and (2) between DOC and dissolved CH₄ concentrations (or CH₄ fluxes)
300 ($p < 0.001$; Figures 5b and S2b).

301 Salinity is another factor that governs CH₄ dynamics in coastal habitats (Segarra et
302 al., 2013; Poffenbarger et al., 2011; Vizza et al., 2017). Higher salinity favors sulfate
303 reducing bacteria over methanogens (Neubauer et al., 2013; Chambers et al., 2013; Vizza
304 et al., 2017), resulting in a lower CH₄ emission (Poffenbarger et al., 2011; Welte et al.,
305 2017; Wilson et al., 2015). Consistent with these earlier observations, during the five-year
306 period of our study, 2017 saw the highest CH₄ diffusive flux, while 2018, 2020 and 2021
307 recorded reduced fluxes (Figure 3d), which corresponded to the interannual rise in salinity

308 of the pond water (Figure 2b) as a result of decline in precipitation (Figure S3). The key
309 role of salinity in regulating CH₄ was also confirmed by our PLS-SEM analysis (Figure
310 6b).

311 Dissolved oxygen often determines the balance between CH₄ production and CH₄
312 oxidation (Bastviken et al., 2008; Liu et al., 2016; Schrier-Uijl et al., 2011). We observed
313 substantial interannual variations in DO (Figure 2d) that mirrored the variations in Chl-*a*
314 (Figure 2h), and DO had strong negative effects on C_{CH_4} and F_{CH_4} (Figures 6b and S2b),
315 suggesting that photosynthetic oxygen production facilitated methane oxidation in the
316 water column.

317 *4.4. Implications for carbon emission assessments and caveats*

318 The escalating need worldwide for protein from aquatic sources has driven the fast
319 expansion of aquaculture ponds, particularly in developing nations (Duan et al., 2020;
320 FAO, 2017; Luo et al., 2022), but aquaculture also causes environmental problems such as
321 nutrient pollution and GHG emissions (Dong et al., 2023b; MacLeod et al., 2020; Yuan et
322 al., 2019). In order to assess the climate impact of coastal aquaculture ponds, we
323 calculated the CO₂+CH₄ combined CO₂-equivalent diffusive flux, which averaged 1,908
324 ± 721 kg CO₂-eq ha⁻¹ yr⁻¹, substantially higher than the average value from China's
325 reservoirs and lakes (Li et al., 2018) and elsewhere (Deemer et al., 2016; Bastviken et al.,
326 2011). Although CH₄ flux (Figure 3d) was lower than CO₂ flux (Figure 3b) in absolute
327 term, the much higher warming potential of CH₄ meant that it accounted for much of the
328 combined CO₂-eq emission (Figure 4). This is different from the result of an earlier
329 meta-analysis, which shows a CO₂:CH₄ flux (CO₂-eq) ratio of > 1 for small ponds

330 (Holgerson and Raymond, 2016). The difference may be explained by the fact that
331 aquaculture ponds are more eutrophic than natural ponds, which tends to favor
332 methanogenesis and increase CH₄ emission. Extrapolating our data to all aquaculture
333 ponds in the coastal region of China (total 1.5×10^4 km²; Duan et al., 2020), we estimated
334 that the combined CO₂-equivalent emissions from these ponds would be equivalent to
335 ~1.5% of the national terrestrial biosphere carbon sink in China ($-2,419$ Tg CO₂-eq yr⁻¹;
336 Wang et al., 2020).

337 Hence, harmonizing economic growth, food security and GHG mitigation from
338 aquaculture systems presents a significant challenge. From our research data, it is evident
339 that the diffusive fluxes of CO₂ and CH₄ from coastal aquaculture ponds decreased with
340 the decline in FCR (Figures 9b and 9d). Enhancing feed utilization efficiency through
341 better feed formulation and management may be pivotal in minimizing GHG emissions
342 from aquaculture ponds, thereby promoting an eco-friendly and sustainable production.

343 In the global effort to combat climate change, proper assessment of GHG emissions
344 from all sectors is required. Although diurnal and seasonal variations of carbon emission
345 from aquaculture ponds have been investigated (e.g., Hu et al., 2020; Yuan et al., 2021;
346 Zhang et al., 2022), most of the studies were limited to a relatively short time period. Our
347 measurements over the five-year period (2017–2021) showed large inter-annual variations,
348 with the coefficient of variation for CO₂ and CH₄ fluxes at 168.0% and 127.3%,
349 respectively. Therefore, short-term or low-frequency measurements could result in large
350 accounting errors in GHG budget.

351 This creates a conundrum for national GHG assessment. Because of the sheer

352 number of small-hold aquaculture ponds spreading over nearly the entire coastline of
353 China, the government simply does not have the resource to monitor them frequently and
354 will have to rely on the farmers to report data on a regular basis, but sophisticated and
355 expensive equipment and procedures are not suitable for small-hold aquaculture operators.
356 Therefore, simple and practical methods for estimating GHG emissions will be highly
357 desirable. Automated or handheld dataloggers for dissolved CO₂ are relatively
358 inexpensive and low maintenance (e.g., Zosel et al., 2011), and F_{CO_2} can be calculated
359 from C_{CO_2} using easily obtained wind (from weather station) and water temperature data
360 (stand-alone sensor or integrated into CO₂ sensor). We therefore attempted to derive
361 useful algorithms to predict F_{CH_4} from F_{CO_2} , and compared the outcomes by binning the
362 data at different time resolutions.

363 Using only the raw data, the linear regressions had poor predictive power ($r^2 < 0.5$),
364 suggesting that CO₂ and CH₄ dynamics in the aquaculture ponds were regulated by
365 different factors there were loosely coupled in time. However, the predictive power of the
366 algorithms improved considerably when we used data averaged by month, by season and
367 by year (Table 1), suggesting that the biogeochemical processes for CO₂ and CH₄ were
368 more in-sync at the lower temporal resolutions. For applications, we recommend
369 measuring C_{CO_2} in high frequency, from which F_{CO_2} can be calculated, then binning F_{CO_2}
370 by month to preserve more temporal detail in the data (Figure 7); monthly F_{CH_4} can then
371 be derived from the algorithm with a fair degree of confidence ($r^2 = 0.664$; $p < 0.001$).

372 Although the algorithm should provide a simple and reliable way to assess total
373 diffusive carbon emission from aquaculture ponds, it is important to consider that this

374 approach did not take into account CH₄ ebullition from the sediment, which at times can
375 be a much larger emission source than diffusion (Yang et al., 2022b). However, ebullition
376 is highly heterogenous in time and in space (de Mello et al., 2018; Martinez and Anderson,
377 2013; Yang et al., 2020b); it cannot be characterized by conventional water sampling or *in*
378 *situ* sensors, and proper measurement would require frequent deployment of gas trap
379 (Yang et al., 2020b) or hydroacoustic detector (Martinez and Anderson, 2013), both of
380 which are not practical for farmers. Devising a simple and reliable method to estimate
381 CH₄ ebullition from aquaculture ponds remains a key challenge to assessing the true
382 extent of climate footprint of the sector.

383 **5. Conclusions**

384 In 2019, the worldwide aquaculture output amounted to 116.8 million tons. FAO
385 (2020) forecasts a 32% surge by 2030, which intensifies concerns about the impact on
386 pollution and climate (Chen et al., 2023; IPCC, 2019). It is a delicate task to balance
387 between economic development, food security and GHG mitigation in the aquaculture
388 sector. Several studies have shown that artificial aeration is a simple and effective method
389 to decrease CH₄ emission from aquaculture ponds, although its adoption among farmers
390 remains limited (Fang et al., 2022; Yang et al., 2023b). We propose that improving feed
391 formulation and refining feed strategies can not only decrease FCR but also cut down
392 carbon emission, leading to a more profitable and sustainable production.

393 This study showed that coastal aquaculture ponds were a strong source for
394 atmospheric CO₂ and CH₄ but with significant temporal variations. As such, short-term or

395 low-frequency measurements may result in erroneous GHG budget. We produced a
396 simple algorithm to derive monthly CH₄ diffusive flux from CO₂ concentration
397 measurements, the latter of which can be monitored routinely with simple sensors and
398 calibrated periodically with more rigorous measurements. This empirical algorithm
399 provides a simple and practical solution that would allow small-hold aquaculture
400 operators and government officials to expand monitoring effort and data coverage to
401 improve GHG assessment.

402

403 **Declaration of competing interest**

404 The authors declare that they have no conflict of interest.

405 **Acknowledgements**

406 The study received collaborative financial support from the National Science
407 Foundation of Fujian Province, China (No. 2022R1002006, and No. 2020J01136) and the
408 National Natural Science Foundation of China (No. 41801070, and No. 41671088).

409 **References**

- 410 Avnimelech, Y., Ritvo, G., 2003. Shrimp and fish pond soils: processes and management.
411 *Aquaculture* 220, 549–567. [https://doi.org/10.1016/S0044-8486\(02\)00641-5](https://doi.org/10.1016/S0044-8486(02)00641-5)
- 412 Bastviken, D., Cole, J.J., Pace, M.L., Van de Bogert, M.C., 2008. Fates of methane from
413 different lake habitats: Connecting whole-lake budgets and CH₄ emissions. *J.*
414 *Geophys. Res.-Biogeo.* 113, G02024. <https://doi.org/10.1029/2007JG000608>
- 415 Bastviken, D., Tranvik, L.J., Downing, J.A., Crill, P.M., Enrich-Prast, A., 2011.
416 Freshwater methane emissions offset the continental carbon sink. *Science* 331, 50.
417 <https://doi.org/10.1126/science.1196808>
- 418 Berberich, M.E., Beaulieu, J.J., Hamilton, T.L., Waldo, S., Buffam, I., 2020. Spatial

419 variability of sediment methane production and methanogen communities within a
420 eutrophic reservoir: Importance of organic matter source and quantity. *Limnol.*
421 *Oceanogr.* 65(6), 1336–1358. <http://dx.doi.org/10.1002/lno.11392>

422 Bernhard, A.E., Peele, E.R., 1997. Nitrogen limitation of phytoplankton in a shallow
423 embayment in northern Puget Sound. *Estuar. Coast.* 20(4), 759–769.
424 <http://dx.doi.org/10.2307/1352249>

425 Bogard, M.J., del Giorgio, P.A., Boutet, L., Chaves, M.C.G., Prairie, Y.T., Merante, A.,
426 Derry, A.M., 2014. Oxic water column methanogenesis as a major component of
427 aquatic CH₄ fluxes. *Nat. Commun.* 5, 5350. <https://doi.org/10.1038/ncomms6350>

428 Borges, A.V., Darchambeau, F., Lambert, T., Bouillon, S., Morana, C., Brouyère, S.,
429 Hakoun, V., Jurado, A., Tseng, H.-C., Descy, J.-P., Roland, F.A.E., 2018. Effects of
430 agricultural land use on fluvial carbon dioxide, methane and nitrous oxide
431 concentrations in a large European river, the Meuse Belgium. *Sci. Total Environ.*
432 610–611, 342–355. <https://doi.org/10.1016/j.scitotenv.2017.08.047>

433 Borges, A.V. Darchambeau, F., Teodoru, C.R., Marwick, T.R., Tamoooh, F., Geeraert, N.,
434 Omengo, F.O., Guérin, F., Lambert, T., Morana, C., Okuku, E., Bouillon, S., 2015.
435 Globally significant greenhouse-gas emissions from African inland waters. *Nat.*
436 *Geosci.* 8, 637–642. <https://doi.org/10.1038/NGEO2486>

437 Boyd, C.E., Wesley Wood, C., Chaney, P.L., Queiroz, J.F., 2010. Role of aquaculture pond
438 sediments in sequestration of annual global carbon emissions. *Environ. Pollut.* 158,
439 2537–2540. <https://doi.org/10.1016/j.envpol.2010.04.025>

440 Chambers, L.G., Osborne, T.Z., Reddy, K.R., 2013. Effect of salinity-altering pulsing
441 events on soil organic carbon loss along an intertidal wetlands gradient: a laboratory
442 experiment. *Biogeochemistry* 115, 363–383.
443 <https://doi.org/10.1007/s10533-013-9841-5>

444 Chanda, A., Das, S., Bhattacharyya, S., Das, I., Giri, S., Mukhopadhyay, A., Samanta, S.,
445 Dutta, D., Akhand, A., Choudhury, S.B., Hazra, S., 2019. CO₂ fluxes from aquaculture
446 ponds of a tropical wetland: Potential of multiple lime treatment in reduction of CO₂
447 emission. *Sci. Total Environ.* 655, 1321–1333.
448 <https://doi.org/10.1016/j.scitotenv.2018.11.332>

449 Chen, Y., Dong, S.L., Wang, Z.N., Wang, F., Gao, Q.F., Tian, X.L., Xiong, Y.H., 2015.
450 Variations in CO₂ fluxes from grass carp *Ctenopharyngodon idella* aquaculture

451 polyculture ponds. *Aquacult. Env. Interac.* 8, 31–40.
452 <https://doi.org/10.3354/aei00149>

453 Chen, Y., Dong, S.L., Wang, F., Gao, Q.F., Tian, X.L., 2016. Carbon dioxide and methane
454 fluxes from feeding and no-feeding mariculture ponds. *Environ. Pollut.* 212, 489–497.
455 <http://dx.doi.org/10.1016/j.envpol.2016.02.039>

456 Chen, G.Z., Bai, J.H., Bi, C., Wang, Y.Q., Cui, B.S., 2023. Global greenhouse gas
457 emissions from aquaculture: a bibliometric analysis. *Agr. Ecosyst. Environ.* 348,
458 108405. <https://doi.org/10.1016/j.agee.2023.108405>

459 Chowdhury, T.R., Dick, R.P., 2013. Ecology of aerobic methanotrophs in controlling
460 methane fluxes from wetlands. *Appl. Soil Ecol.* 65, 8–22.
461 <https://doi.org/10.1016/j.apsoil.2012.12.014>

462 Cotovicz Jr., L.C., Knoppers, B.A., Brandini, N., Poirier, D., Costa Santos, S.J., Abril, G.,
463 2016. Spatio-temporal variability of methane (CH₄) concentrations and diffusive
464 fluxes from a tropical coastal embayment surrounded by a large urban area
465 (Guanabara Bay, Rio de Janeiro, Brazil). *Limnol. Oceanogr.* 61(S1), S238–S252.
466 <https://doi.org/10.1002/lno.10298>

467 Cole, J.J., Caraco, N.F., 1998. Atmospheric exchange of carbon dioxide in a low-wind
468 oligotrophic lake measured by the addition of SF₆. *Limnol. Oceanogr.* 43(4), 647–656.
469 <https://doi.org/10.4319/lo.1998.43.4.0647>

470 Crusius, J., Wanninkhof, R., 2003. [Gas transfer velocities measured at low wind speed](https://doi.org/10.4319/lo.2003.48.3.1010)
471 [over a lake. *Limnol. Oceanogr.* 48\(3\), 1010–1017.](https://doi.org/10.4319/lo.2003.48.3.1010)

472 Davidson, T.A., Audet, J., Jeppesen, E., Landkildehus, F., Lauridsen, T.L., Søndergaard,
473 M., Syväranta, J., 2018. Synergy between nutrients and warming enhances methane
474 ebullition from experimental lakes. *Nat. Clim. Change* 8(2), 156.
475 <https://doi.org/10.1038/s41558-017-0063-z>

476 Deemer, B.R., Harrison, J.A., Li, S.Y., Beaulieu, J.J., Delsontro, T., Barros, N.,
477 BezerraNeto, J.F., Powers, S.M., Santos, M.A.D., Vonk, J.A., 2016. Greenhouse gas
478 emissions from reservoir water surfaces: a new global synthesis. *Bioscience* 66,
479 949–964. <https://doi.org/10.1093/biosci/biw117>

480 de Mello, N.A.S.T., Brighenti, L.S., Barbosa, F.A.R., Staehr, P.A., Bezerra Neto, J.F.,
481 2018. Spatial variability of methane (CH₄) ebullition in a tropical hypereutrophic
482 reservoir: silted areas as a bubble hot spot. *Lake Reserv. Manage.* 34(2), 105–114.

483 <https://doi.org/10.1080/10402381.2017.1390018>

484 Dong, Y.H., Yuan, J.J., Li, J.J., Liu, D.Y., Qiu, Y., Zhang, X., Xiang, J., Ding, W.X., 2023a.
485 Conversion of natural coastal wetlands to mariculture ponds dramatically decreased
486 methane production by reducing substrate availability. *Agr. Ecosyst. Environ.* 356,
487 108646. <https://doi.org/10.1016/j.agee.2023.108646>

488 Dong, B.G., Xi, Y., Cui, Y.X., Peng, S.S., 2023b. Quantifying methane emissions from
489 aquaculture ponds in China. *Environ. Sci. Technol.* 57(4), 1576–1583.
490 <https://doi.org/10.1021/acs.est.2c05218>

491 Downing, J.A., 2010. Emerging global role of small lakes and ponds: little things mean a
492 lot. *Limnetica*, 29, 9–23. <https://doi.org/10.1899/09-028.1>

493 Duan, Y.Q., Li, X., Zhang, L.P., Chen, D., Liu, S.A., Ji, H.Y., 2020. Mapping
494 national-scale aquaculture ponds based on the Google Earth Engine in the Chinese
495 coastal zone. *Aquaculture* 520, 734666.
496 <https://doi.org/10.1016/j.aquaculture.2019.734666>

497 FAO, 2017. Fishery and aquaculture statistics (global aquaculture production 1950–2014).
498 *FishStatJ*. <http://www.fao.org/fishery/statistics/software/fishstatj/en>

499 FAO, 2020. The State of World Fisheries and Aquaculture 2020. Sustainability in action.
500 Rome. <https://doi.org/10.4060/ca9229en>

501 Fang, X.T., Wang, C., Zhang, T.R., Zheng, F.W., Zhao, J.T., Wu, S., Barthel, M., Six, J.,
502 Zou, J.W., Liu, S.W., 2022. Ebullitive CH₄ flux and its mitigation potential by aeration
503 in freshwater aquaculture: Measurements and global data synthesis. *Agr. Ecosyst.*
504 *Environ.* 335, 108016. <https://doi.org/10.1016/j.agee.2022.108016>

505 Flickinger, D.L., Costa, G.A., Dantas, D.P., Proença, D.C., David, F.S., Durborow, R.M.,
506 Moraes-Valentia, P., Valenti, W.C., 2020. The budget of carbon in the farming of the
507 Amazon river prawn and tambaqui fish in earthen pond monoculture and integrated
508 multitrophic systems. *Aquacult. Rep.* 17, 100340.
509 <https://doi.org/10.1016/j.aqrep.2020.100340>

510 Friedlingstein, P., O'Sullivan, M., Jones, M.W., Andrew, R.M., Gregor, L., et al., 2022
511 Global Carbon Budget 2022. *Earth Syst. Sci. Data* 14, 4811–4900.
512 <https://doi.org/10.5194/essd-14-4811-2022>

513 Gao, D.Z., Liu, M., Hou, L.J., Lai, D.Y.F., Wang, W.Q., Li, X.F., Zeng, A.Y., Zheng, Y.L.,
514 Han, P., Yang, Y., Yin, G.Y., 2019. Effects of shrimp-aquaculture reclamation on

515 sediment nitrate dissimilatory reduction processes in a coastal wetland of southeastern
516 China. *Environ. Pollut.* 255, 113219. <https://doi.org/10.1016/j.envpol.2019.113219>

517 Gruca-Rokosz, R., Szal, D., Bartoszek, L., Pękala, A., 2020. Isotopic evidence for vertical
518 diversification of methane production pathways in freshwater sediments of Nielisz
519 reservoir (Poland). *Catena* 195, 104803. <https://doi.org/10.1016/j.catena.2020.104803>

520 Gudas, C., Bastviken, D., Steger, K., Premke, K., Sobek, S., Tranvik, L.J., 2010.
521 Temperature-controlled organic carbon mineralization in lake sediments. *Nature* 466,
522 478–482. <https://doi.org/10.1038/nature09186>

523 Holgerson, M.A., 2015. Drivers of carbon dioxide and methane supersaturation in small,
524 temporary ponds. *Biogeochemistry* 124(1–3), 305–318.
525 <https://doi.org/10.1007/s10533-015-0099-y>

526 Holgerson, M.A., Raymond, P.A., 2016. Large contribution to inland water CO₂ and CH₄
527 emissions from very small ponds. *Nat. Geosci.* 9(3), 222–226.
528 <https://doi.org/10.1038/ngeo2654>

529 Hu, B.B., Xu, X.F., Zhang, J.F., Wang, T.L., Meng, W.Q., Wang, D.Q., 2020. Diurnal
530 variations of greenhouse gases emissions from reclamation mariculture ponds. *Estuar.
531 Coast. Shelf S.* 237, 106677. <https://doi.org/10.1016/j.ecss.2020.106677>

532 Huttunen, J.T., Alm, J., Liikanen, A., Juutinen, S., Larmola, T., Hammar, T., Silvola, J.,
533 Martikainen, P.J., 2003. Fluxes of methane, carbon dioxide and nitrous oxide in boreal
534 lakes and potential anthropogenic effects on the aquatic greenhouse gas emissions.
535 *Chemosphere* 52, 609–621. [https://doi.org/10.1016/s0045-6535\(03\)00243-1](https://doi.org/10.1016/s0045-6535(03)00243-1)

536 IPCC, 2019. In: Calvo Buendia, E., Tanabe, K., Kranjc, A., Baasansuren, J., Fukuda, M.,
537 Ngarize, S. (Eds.), 2019 Refinement to the 2006 IPCC Guidelines for National
538 Greenhouse Gas Inventories, Volum 4. IPCC, Switzerland. Kanagawa, Japan Chapter
539 07.

540 Jensen, S.A., Webb, J.R., Simpson, G.L., Baulch, H.M., Leavitt, P.R., Finlay, K., 2023.
541 Differential controls of greenhouse gas (CO₂, CH₄, and N₂O) concentrations in natural
542 and constructed agricultural waterbodies on the Northern Great Plains. *J. Geophys.
543 Res.-Biogeo.* 128, e2022JG007261. <https://doi.org/10.1029/2022JG007261>

544 Jia, J.J., Sun, K., Lü, S.D., Li, M.X., Wang, Y.F., Yu, G.R., Gao, Y., 2022. Determining
545 whether Qinghai–Tibet Plateau waterbodies have acted like carbon sinks or sources
546 over the past 20 years. *Sci. Bull.* 67, 2345–2357.

547 <https://doi.org/10.1016/j.scib.2022.10.023>

548 Kang, L.J., Zhu, G.W., Zhu, M.Y., Xu, H., Zou, W., Xiao, M., Zhang, Y.L., Qin, B.Q.,
549 2023. Bloom-induced internal release controlling phosphorus dynamics in large
550 shallow eutrophic Lake Taihu, China. *Environ. Res.* 231(Part 3), 116251.
551 <https://doi.org/10.1016/j.envres.2023.116251>

552 Kosten, S., Almeida, R.M., Barbosa, I., Mendonç, R., Muzitano, I.S., Oliveira-Junior, E.S.,
553 Vroom, R.J.E., Wang, H.J., Barros, N., 2020. Better assessments of greenhouse gas
554 emissions from global fish ponds needed to adequately evaluate aquaculture footprint.
555 *Sci. Total Environ* 748, 141247. <https://doi.org/10.1016/j.scitotenv.2020.141247>

556 Lapointe, B.E., Herren, L.W., Debortoli, D.D., Vogel, M.A., 2015. Evidence of
557 sewage-driven eutrophication and harmful algal blooms in Florida's Indian River
558 Lagoon. *Harmful Algae* 43, 82–102. <http://dx.doi.org/10.1016/j.hal.2015.01.004>

559 Le Quéré, C., Andrew, R.M., Friedlingstein, P., Sitch, S., Hauck, J., et al., 2018. Global
560 Carbon Budget 2018. *Earth Syst. Sci. Data* 10, 2141–2194.
561 <https://doi.org/10.5194/essd-10-2141-2018>.

562 Li, S.Y., Bush, R.T., Santos, I.R., Zhang, Q.F., Song, K.S., Mao, R., Wen, Z.D., Lu, X.X.,
563 2018. Large greenhouse gases emissions from China's lakes and reservoirs. *Water Res.*
564 147, 13–24. <https://doi.org/10.1016/j.watres.2018.09.053>.

565 Lin, G.M., Lin, X.B., 2022. Bait input altered microbial community structure and
566 increased greenhouse gases production in coastal wetland sediment. *Water Res.* 218,
567 118520. <https://doi.org/10.1016/j.watres.2022.118520>

568 Liu, S.W., Hu, Z.Q., Wu, S., Li, S.Q., Li, Z.F., Zou, J.W., 2016. Methane and nitrous
569 oxide emissions reduced following conversion of rice paddies to inland crab-fish
570 aquaculture in southeast China. *Environ. Sci. Technol.* 50(2), 633–642.
571 <https://doi.org/10.1021/acs.est.5b04343>

572 Liu, Z.H., Dreybrodt, W., Wang, H.J., 2010. A new direction in effective accounting for
573 the atmospheric CO₂ budget: considering the combined action of carbonate
574 dissolution, the global water cycle and photosynthetic uptake of DIC by aquatic
575 organisms. *Earth Sci. Rev.* 99, 162–172.
576 <https://doi.org/10.1016/j.earscirev.2010.03.001>

577 Luo, J.H., Sun, Z., Lu, L.R., Xiong, Z.Y., Cui, L.P., Mao, Z.G., 2022. Rapid expansion of
578 coastal aquaculture ponds in Southeast Asia: Patterns, drivers and impacts. *J. Environ.*

579 Manage. 315, 115100. <https://doi.org/10.1016/j.jenvman.2022.115100>

580 MacLeod, M.J., Hasan, M.R., Robb, D.H., Mamun-Ur-Rashid, M., 2020. Quantifying
581 greenhouse gas emissions from global aquaculture. *Sci. Rep.* 10(1), 11679.
582 <https://doi.org/10.1038/s41598-020-68231-8>

583 Martinez, D., Anderson, M. A., 2013. Methane production and ebullition in a shallow,
584 artificially aerated, eutrophic temperate lake (Lake Elsinore, CA). *Sci. Total*
585 *Environ.* 454, 457–465. <https://doi.org/10.1016/j.scitotenv.2013.03.040>

586 Marescaux, A., Thieu, V., Garnier, J., 2018. Carbon dioxide, methane and nitrous oxide
587 emissions from the human-impacted Seine watershed in France. *Sci. Total Environ.*
588 643, 247–259. <https://doi.org/10.1016/j.scitotenv.2018.06.151>

589 Molnar, N., Welsh, D.T., Marchand, C., Deborde, J., Meziane, T., 2013. Impacts of shrimp
590 farm effluent on water quality, benthic metabolism and N-dynamics in a mangrove
591 forest (New Caledonia). *Estuar. Coast. Shelf S.* 117, 12–21.
592 <https://doi.org/10.1016/j.ecss.2012.07.012>

593 Musenze, R.S., Grinham, A., Werner, U., Gale, D., Sturm, K., Udy, J., Yuan, Z.G., 2014.
594 Assessing the spatial and temporal variability of diffusive methane and nitrous oxide
595 emissions from subtropical freshwater reservoirs. *Environ. Sci. Technol.* 48,
596 14499–14507. <https://doi.org/10.1021/es505324h>

597 Myhre, G., Shindell, D., Breon, F.M., Collins, W., Fuglestedt, J., Huang, J., Koch, D.,
598 Lamarque, J.F., Lee, D., Mendoza, B., Nakajima, T., Robock, A., Stephens, G.,
599 Takemura, T., Zhang, H., 2013. *Anthropogenic and natural radiative forcing. In:*
600 *climate change 2013, the physical science basis. Contribution of working group i to*
601 *the fifth assessment report of the intergovernmental panel on climate change,*
602 *Cambridge University Press, Cambridge.*

603 Natchimuthu, S., Sundgren, I., Gålfalk, M., Klemedtsson, L., Crill, P., Danielsson, Å.,
604 Bastviken, D., 2016. Spatio-temporal variability of lake CH₄ fluxes and its influence
605 on annual whole lake emission estimates. *Limnol. Oceanogr.* 61(S1), S13–S26.
606 <https://doi.org/10.1002/lno.10222>

607 National Oceanic and Atmospheric (NOAA), 2023. Carbon cycle greenhouse gases.
608 Available in: <https://www.esrl.noaa.gov/gmd/ccgg/>

609 Naylor, R.L., Hardy, R.W., Buschmann, A.H., Bush, S.R., Cao, L., Klinger, D.H., Little,
610 D.C., Lubchenco, J., Shumway, S.E., Troell, M., 2021. A 20-year retrospective review

611 of global aquaculture. Nature 591, 551–563.
612 <https://doi.org/10.1038/s41586-021-03308-6>

613 Neubauer, S.C., Franklin, R.B., Berrier, D.J., 2013. Saltwater intrusion into tidal
614 freshwater marshes alters the biogeochemical processing of organic carbon.
615 Biogeosciences 10, 8171–8183. <https://doi.org/10.5194/bg-10-8171-2013>

616 Neubauer, S.C., Megonigal, J.P., 2019. Correction to: Moving beyond global warming
617 potentials to quantify the climatic role of ecosystems. Ecosystems 22, 1931–1932.
618 <https://doi.org/10.1007/s10021-019-00422-5>.

619 Peacock, M., Audet, J., Bastviken, D., Cook, S., Futter, M.N., 2021. Small artificial
620 waterbodies are widespread and persistent emitters of methane and carbon dioxide.
621 Global Change Biol. 27, 5109–5123. <https://doi.org/10.1111/gcb.15762>

622 Pouil, S., Samsudin, R., Slembrouck, J., Sihabuddin, A., Sundari, G., Khazaidan, K.,
623 Kristanto, A.H., Pantjara, B., Caruso, D., 2019. Nutrient budgets in a small-scale
624 freshwater fish pond system in Indonesia. Aquaculture 504, 267–274.
625 <https://doi.org/10.1016/j.aquaculture.2019.01.067>

626 Praetzel, L.S.E., Schmiedeskamp, M., Knorr, K.H., 2021. Temperature and sediment
627 properties drive spatiotemporal variability of methane ebullition in a small and
628 shallow temperate lake. Limnol. Oceanogr. 66(7), 2598–2610.
629 <https://doi.org/10.1002/lno.11775>

630 Prėskienis, V., Laurion, I., Bouchard, F., Douglas, P.M.J., Billett, M.F., Fortier, D., Xu,
631 X.M., 2021. Seasonal patterns in greenhouse gas emissions from lakes and ponds in a
632 High Arctic polygonal landscape. Limnol. Oceanogr. 66, S117–S141.
633 <https://doi.org/10.1002/lno.11660>

634 Raymond, P.A., Hartmann, J., Lauerwald, R., Sobek, S., McDonald, C., Hoover, M.,
635 Butman, D., Striegl, R., Mayorga, E., Humborg, C., Kortelainen, P., Duerr, H.,
636 Meybeck, M., Ciais, P., Guth, P., 2013. Global carbon dioxide emissions from inland
637 waters. Nature 503(7476), 355–359. <https://doi.org/10.1038/nature12760>

638 Rubbo, M., Cole, J., Kiesecker, J., 2006. Terrestrial subsidies of organic carbon support
639 net ecosystem production in temporary forest ponds: evidence from an ecosystem
640 experiment. Ecosystems 9, 1170–1176. <https://doi.org/10.1007/s10021-005-0009-6>

641 Sahu, B.C., Adhikari, S., Mahapatra, A.S., Dey, L., 2013. Carbon, nitrogen, and
642 phosphorus budget in scampi (*Macrobrachium rosenbergii*) culture ponds. Environ.

643 Monit. Assess. 185, 10157–10166. <https://doi.org/10.1007/s10661-013-3320-2>

644 Segarra, K.E.A., Comerford, C., Slaughter, J., Joye, S.B., 2013. Impact of electron
645 acceptor availability on the anaerobic oxidation of methane in coastal freshwater and
646 brackish wetland sediments. *Geochimi. Cosmochimi. Ac.* 115, 15–30.
647 <https://doi.org/10.1016/j.gca.2013.03.029>

648 Segers, R., 1998. Methane production and methane consumption: a review of processes
649 underlying wetland methane fluxes. *Biogeochemistry* 41, 23–51.
650 <https://doi.org/10.1023/A:1005929032764>

651 Schrier-Uijl, A.P., Veraart, A.J., Leffelaar, P.A., Berendse, F., Veenendaal, E.M., 2011.
652 Release of CO₂ and CH₄ from lakes and drainage ditches in temperate wetlands.
653 *Biogeochemistry*, 102(1-3), 265–279. <https://doi.org/10.1007/s10533-010-9440-7>

654 Poffenbarger, H.J., Needelman, B.A., Megonigal, J.P., 2011. Salinity influence on
655 methane emissions from tidal marshes. *Wetlands* 31, 831–842.
656 <https://doi.org/10.1007/s13157-011-0197-0>

657 Tan, L.S., Ge, Z.M., Ji, Y.H., Lai, D.Y.F., Temmerman, S., Li, S.H., Li, X.Z., Tang, J.W.,
658 2022. Land use and land cover changes in coastal and inland wetlands cause soil
659 carbon and nitrogen loss. *Global Ecol. Biogeogr.* 31, 2541–2563.
660 <https://doi.org/10.1111/geb.13597>

661 Tan, L.S., Zhang, L.H., Yang, P., Tong, C., Lai, D.Y.F., Yang, H., Hong, Y., Tian, Y.L.,
662 Tang, C., Ruan, M.J., Tang, K.W., 2023. Effects of conversion of coastal marshes to
663 aquaculture ponds on sediment anaerobic CO₂ production and emission in a
664 subtropical estuary of China. *J. Environ. Manage.* 338, 117813.
665 <https://doi.org/10.1016/j.jenvman.2023.117813>

666 Tang, K.W., McGinnis, D.F., Ionescu, D., Grossart, H.-P., 2016. Methane production in
667 oxic lake waters potentially increases aquatic methane flux to air. *Environ. Sci.*
668 *Technol. Lett.* 3 (6), 227–233. <http://dx.doi.org/10.1021/acs.estlett.6b00150>

669 Tian, Y.L., Yang, P., Yang, H., Wang, H.M., Zhang, L.H., Tong, C., Lai, D.Y.F., Lin, Y.X.,
670 Tan, L.S., Hong, Y., Tang, C., Tang, K.W., 2023. Diffusive nitrous oxide (N₂O) fluxes
671 across the sediment-water-atmosphere interfaces in aquaculture shrimp ponds in a
672 subtropical estuary: Implications for climate warming. *Agr. Ecosyst. Environ.* 341,
673 108218. <https://doi.org/10.1016/j.agee.2022.108218>

674 Tong, C., Morris, J.T., Huang, J.F., Xu, H., Wan, S.A., 2018. Changes in pore-water

675 chemistry and methane emission following the invasion of *Spartina alterniflora* into
676 an oligohaline marsh. *Limnol. Oceanogr.* 63, 384–396.
677 <https://doi.org/10.1002/lno.10637>

678 Tong, C., Bastviken, D., Tang, K.W., Yang, P., Yang, H., Zhang, Y.F., Guo, Q.Q., Lai,
679 D.Y.F., 2020. Annual CO₂ and CH₄ fluxes in coastal earthen ponds with *Litopenaeus*
680 *vannamei* in southeastern China. *Aquaculture* 545, 737229.
681 <https://doi.org/10.1016/j.aquaculture.2021.737229>

682 Vizza, C., West, W.E., Jones, S.E., Hart, J.A., Lamberti, G.A., 2017. Regulators of coastal
683 wetland methane production and responses to simulated global change.
684 *Biogeosciences* 14(2), 431–446. <https://doi.org/10.5194/bg-14-431-2017>

685 Wang, F.S., Lang, Y.C., Liu, C.Q., Qin, Y., Yu, N.X., Wang, B.L., 2019. Flux of organic
686 carbon burial and carbon emission from a large reservoir: implications for the
687 cleanliness assessment of hydropower. *Sci. Bull.* 64, 603–611.
688 <https://doi.org/10.1016/j.scib.2019.03.034>

689 Wang, J., Feng, L., Palmer, P.I., Liu, Y., Fang, S., Bsch, H., O'Dell, C.W., Tang, X.P.,
690 Yang, D.X., Liu, L.X., Xia, C.Z., 2020. Large Chinese land carbon sink estimated
691 from atmospheric carbon dioxide data. *Nature* 586, 720–723.
692 <https://doi.org/10.1038/s41586-020-2849-9>

693 Wang, M., Mao, D.H., Xiao, X.M., Song, K.S., Jia, M.M., Ren, C.Y., Wang, Z.M., 2023.
694 Interannual changes of coastal aquaculture ponds in China at 10-m spatial resolution
695 during 2016–2021. *Remote Sens. Environ.* 284, 113347.
696 <https://doi.org/10.1016/j.rse.2022.113347>

697 Wanninkhof, R., 1992. Relationship between wind-speed and gas-exchange over the
698 ocean. *J. Geophys. Res.-Oceans* 97, 7373–7382. <https://doi.org/10.1029/92jc00188>.

699 Welti, N., Hayes, M., Lockington, D., 2017. Seasonal nitrous oxide and methane
700 emissions across a subtropical estuarine salinity gradient. *Biogeochemistry* 132(1-2),
701 55–69. <https://doi.org/10.1007/s10533-016-0287-4>

702 Wilson, B.J., Mortazavi, B., Kiene, R.P., 2015. Spatial and temporal variability in carbon
703 dioxide and methane exchange at three coastal marshes along a salinity gradient in a
704 northern Gulf of Mexico estuary. *Biogeochemistry* 123(3), 329–347.
705 <https://doi.org/10.1007/s10533-015-0085-4>

706 Xiao, Q.T., Duan, H.T., Qi, T.C., Hu, Z.H., Liu, S.D., Zhang, M., Lee, X.H., 2020.

707 Environmental investments decreased partial pressure of CO₂ in a small eutrophic
708 urban lake: Evidence from long-term measurements. *Environ. Pollut.* 263, 114433.
709 <https://doi.org/10.1016/j.envpol.2020.114433>

710 Xu, H., Paerl, H.W., Zhu, G.W., Qin, B.Q., Hall, N.S., Zhu, M.Y., 2017. Long-term
711 nutrient trends and harmful cyanobacterial bloom potential in hypertrophic Lake Taihu,
712 China. *Hydrobiologia* 787, 229–242. <https://doi.org/10.1007/s10750-016-2967-4>

713 Yang, G.B., Zheng, Z.H., Abbott, B.W., Olefeldt, D.,Knoblauch, C., Song, Y.T., Kang,
714 L.Y., Qin, S.Q., Peng, Y.F., Yang, Y.H., 2023a. Characteristics of methane emissions
715 from alpine thermokarst lakes on the Tibetan Plateau. *Nat. Commun.* 14, 3121.
716 <https://doi.org/10.1038/s41467-023-38907-6>

717 Yang, H., Huang, X., Hu, J., Thompson, J. R., Flower, R. J. 2022a. Achievements,
718 challenges and global implications of China’s carbon neutral pledge. *Front. Env. Sci.*
719 *Eng.* 16(8), 111. <https://doi.org/10.1007/s11783-022-1532-9>

720 Yang, P., Yang, H., Sardans, J., Tong, C., Zhao, G.H., Peñuelas, J., Ling Li, Zhang, Y.F.,
721 Tan, L.S., Chun, K.P., Lai, D.Y.F., 2020a. Large spatial variations in diffusive CH₄
722 fluxes from a subtropical coastal reservoir affected by sewage discharge in southeast
723 China. *Environ. Sci. Technol.* 54 (22), 14192–14203.
724 <https://doi.org/10.1021/acs.est.0c03431>

725 Yang, P., Zhang, Y.F., Yang, H., Guo, Q.Q., Lai, D.Y.F., Zhao, G.H., Li, L., Tong, C.,
726 2020b. Ebullition was a major pathway of methane emissions from the aquaculture
727 ponds in southeast China. *Water Res.* 184, 116176.
728 <https://doi.org/10.1016/j.watres.2020.116176>.

729 Yang, P., Lai, D.Y.F., Yang, H., Lin, Y.X., Tong, C., Hong, Y., Tian, Y.L., Tang, C., Tang,
730 K.W., 2022b. Large increase in CH₄ emission following conversion of coastal marsh
731 to aquaculture ponds caused by changing gas transport pathways. *Water Res.* 222,
732 118882. <https://doi.org/10.1016/j.watres.2022.118882>

733 Yang, P., Lai, D.Y.F., Yang, H., Tong, C., 2019. Carbon dioxide dynamics from sediment,
734 sediment-water interface and overlying water in the aquaculture shrimp ponds in
735 subtropical estuaries, southeast China. *J. Environ. Manage.* 236, 224–235.
736 <https://doi.org/10.1016/j.jenvman.2019.01.088>

737 Yang, P., Tang, K.W., Yang, H., Tong, C., Zhang, L.H., Lai, D.Y.F., Hong, Y., Tan, L.S.,
738 Zhu, W.Y., Tang, C., 2023b. Contrasting effects of aeration on methane (CH₄) and

739 nitrous oxide (N₂O) emissions from subtropical aquaculture ponds and implications
740 for global warming mitigation. *J. Hydrol.* 617, 128876.
741 <https://doi.org/10.1016/j.jhydrol.2022.128876>

742 Yuan, J.J., Xiang, J., Liu, D.Y., Kang, H., He, T.H., Kim, S., Lin, Y.X., Freeman, C., Ding,
743 W.X., 2019. Rapid growth in greenhouse gas emissions from the adoption of
744 industrial-scale aquaculture. *Nat. Clim. Change* 9(4), 318–322.
745 <https://doi.org/10.1038/s41558-019-0425-9>

746 Yuan, J.J., Liu, D.Y., Xiang, J., He, T.H., Kang, H., Ding, W.X., 2021. Methane and
747 nitrous oxide have separated production zones and distinct emission pathways in
748 freshwater aquaculture ponds. *Water Res.* 190, 116739.
749 <https://doi.org/10.1016/j.watres.2020.116739>

750 Zabranska, J., Pokorna, D., 2018. Bioconversion of carbon dioxide to methane using
751 hydrogen and hydrogenotrophic methanogens. *Biotechnol. Adv.* 36(3), 707–720.
752 <https://doi.org/10.1016/j.biotechadv.2017.12.003>

753 Zhang, K., Xie, J., Yu, D.G., Wang, G.J., Yu, E.M., Gong, W.B., Li, Z.F., Wang, C.C., Xia,
754 Y., 2018. A comparative study on the budget of nitrogen and phosphorus in
755 polyculture systems of snakehead with bighead carp. *Aquaculture* 483, 69–75.
756 <http://dx.doi.org/10.1016/j.aquaculture.2017.10.004>

757 Zhang, Y.F., Lyu, M., Yang, P., Lai, D.Y.F., Tong, C., Zhao, G.H., Li, L., Zhang, Y.H.,
758 Yang, H., 2021. Spatial variations in CO₂ fluxes in a subtropical coastal reservoir of
759 Southeast China were related to urbanization and land-use types. *J. Environ. Sci.* 109,
760 206–218. <https://doi.org/10.1016/j.jes.2021.04.003>

761 Zhang, Y.P., Qin, Z.C., Li, T.T., Zhu, X.D., 2022. Carbon dioxide uptake overrides
762 methane emission at the air-water interface of algae-shellfish mariculture ponds:
763 Evidence from eddy covariance observations. *Sci. Total Environ.* 815, 152867.
764 <https://doi.org/10.1016/j.scitotenv.2021.152867>

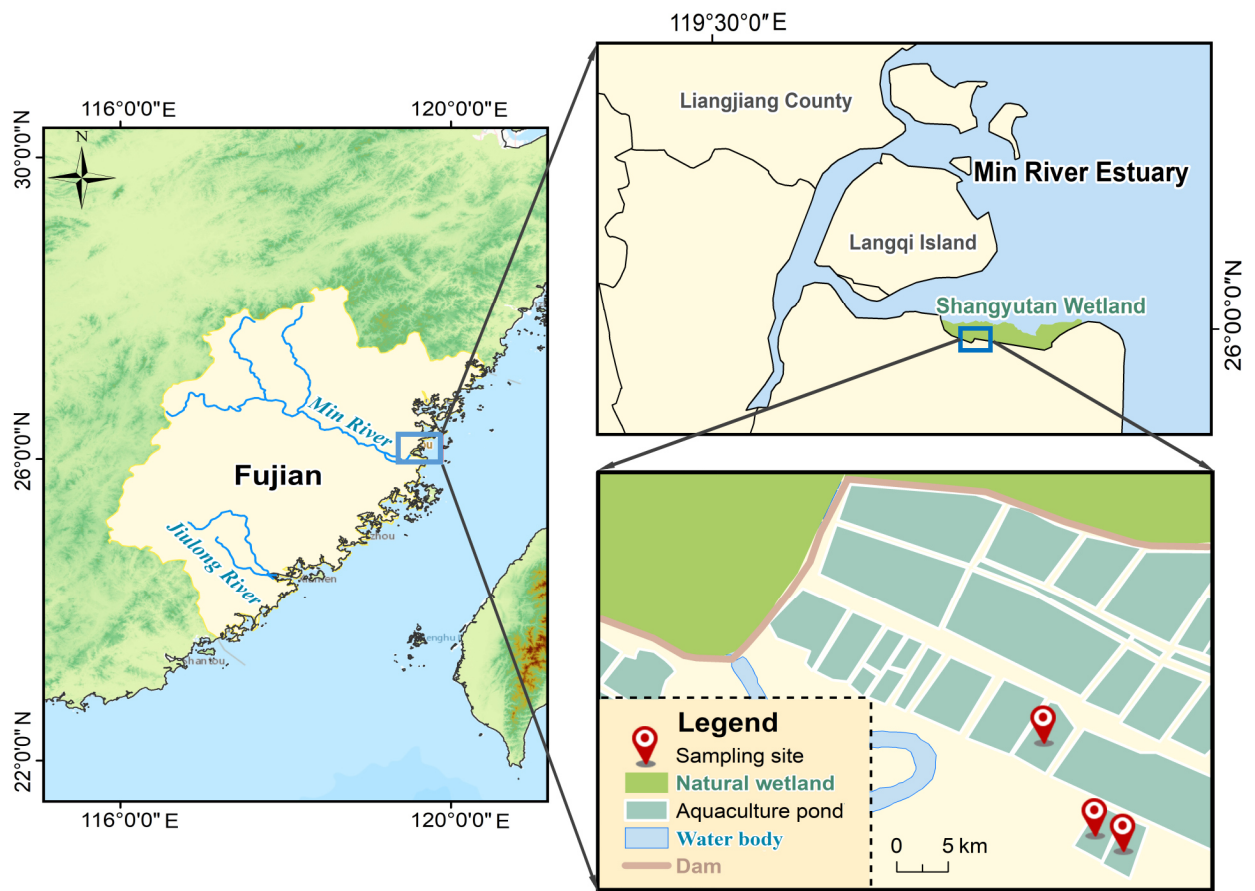
765 Zhao, J.Y., Zhang, M., Xiao, W., Jia, L., Zhang, X.F., Wang, J., Zhang, Z., Xie, Y.H., Pu, Y.
766 N., Liu, S.D., Feng, Z.Z., Lee, X.H., 2021. Large methane emission from freshwater
767 aquaculture ponds revealed by long-term eddy covariance observation. *Agr. Forest.*
768 *Meteorol.* 308–309, 108600. <https://doi.org/10.1016/j.agrformet.2021.108600>

769 Zhou, Y.Q., Xiao, Q.T., Yao, X.L., Zhang, Y.L., Zhang, M., Shi, K., Lee, X.H., Podgorski,
770 D.C., Qin, B.Q., Spencer, R.G.M. Jeppesen, E., 2018. Accumulation of terrestrial

771 dissolved organic matter potentially enhances dissolved methane levels in eutrophic
772 Lake Taihu, China. *Environ. Sci. Technol.* 52(18), 10297–10306.
773 <https://doi.org/10.1021/acs.est.8b02163>
774 Zosel, J., Oelßner, W., Decker, M., Gerlach, G., Guth, U., 2011. The measurement of
775 dissolved and gaseous carbon dioxide concentration. *Meas. Sci. Technol.* 22(7),
776 072001. <https://doi.org/10.1088/0957-0233/22/7/072001>

Table 1 Linear regression analysis with CO₂ concentration (C_{CO_2} ; $\mu\text{mol L}^{-1}$) or flux (F_{CO_2} ; $\text{mmol m}^{-2} \text{h}^{-1}$) as independent variable (x); CH₄ concentration (C_{CH_4} ; $\mu\text{mol L}^{-1}$) or flux (F_{CH_4} ; $\mu\text{mol m}^{-2} \text{h}^{-1}$) as predicted variable (y). Regressions were run using all data without binning, data binned (averaged) by month, by season or by year. Outputs include y -intercept, slope, standard error of slope, r^2 and p values of the regressions.

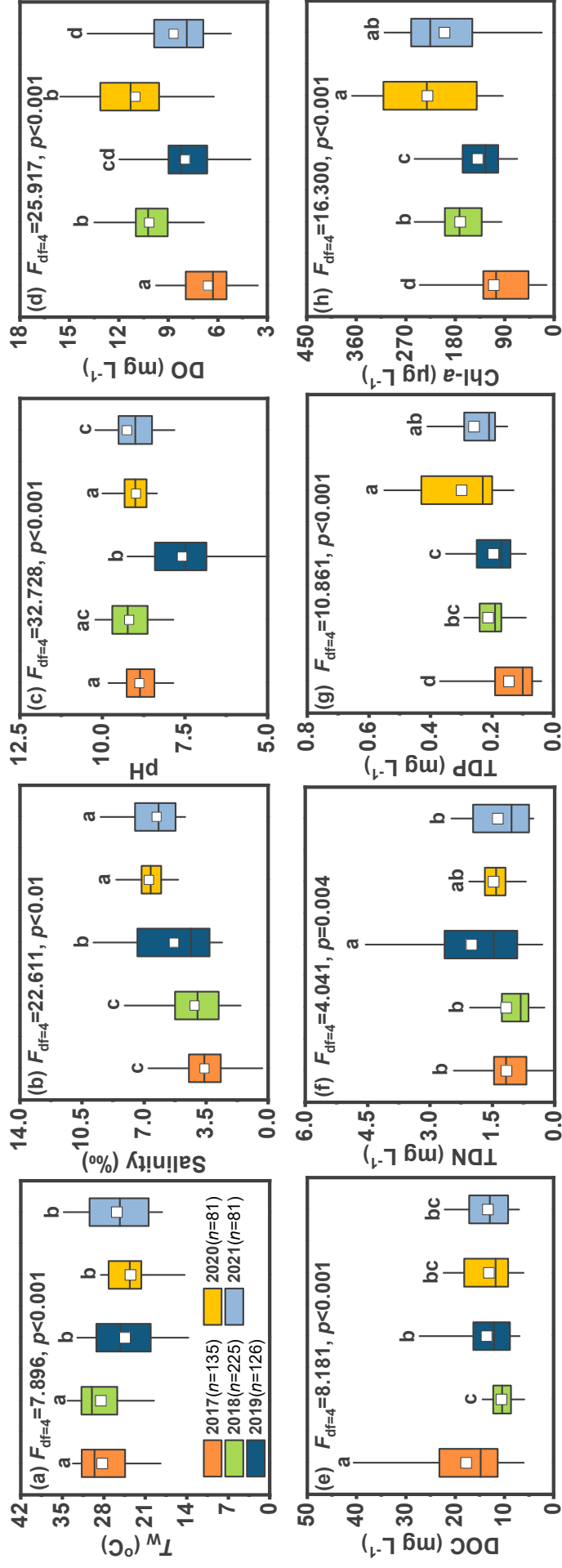
x	y	Intercept	Slope	Slope SE	r^2	p
<i>All data</i>						
C_{CO_2}	C_{CH_4}	0.969	0.030	0.016	0.018	0.065
F_{CO_2}	F_{CH_4}	25.293	68.279	9.869	0.206	0.000
<i>Monthly</i>						
C_{CO_2}	C_{CH_4}	-0.605	0.098	0.025	0.310	0.000
F_{CO_2}	F_{CH_4}	11.782	101.848	12.428	0.664	0.000
<i>Seasonal</i>						
C_{CO_2}	C_{CH_4}	-0.959	0.119	0.036	0.454	0.006
F_{CO_2}	F_{CH_4}	13.064	107.174	17.016	0.753	0.000
<i>Yearly</i>						
C_{CO_2}	C_{CH_4}	-1.681	0.154	0.025	0.927	0.009
F_{CO_2}	F_{CH_4}	11.973	102.653	10.609	0.969	0.002



1

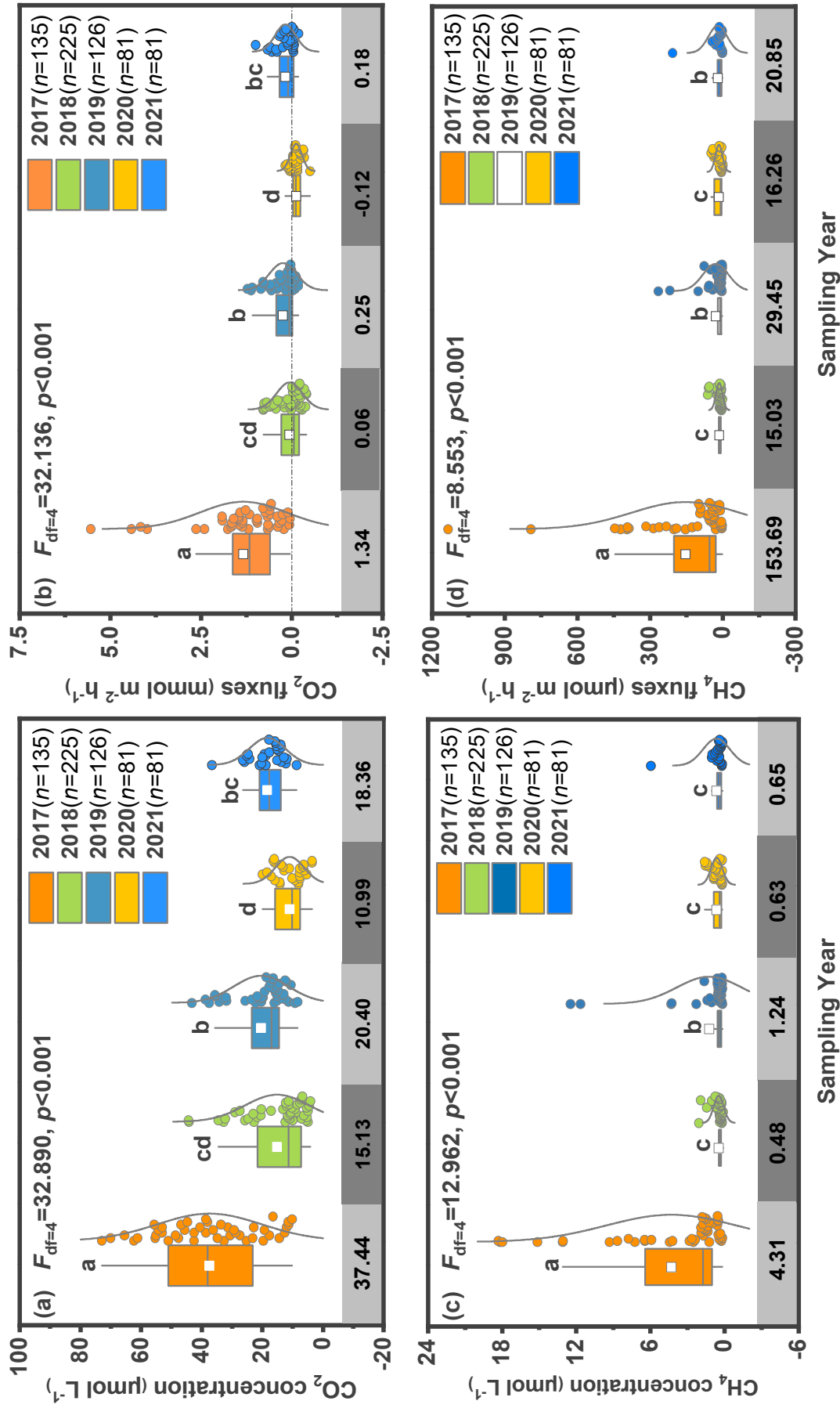
2 **Figure 1** Locations of the study areas and sampling sites in Shanyutan Wetland within the

3 Min River Estuary, Fujian Province, southeast China.



4

5 **Figure 2** Box plots of (a) water temperature (T_w), (b) salinity, (c) pH, (d) dissolved organic carbon (DOC), (e) total
6 dissolved nitrogen (TDN), (g) total dissolved phosphorus (TDP) and (h) chlorophyll-*a* (Chl-*a*) in surface water for coastal aquaculture ponds over a
7 five-year period. Different letters above the boxes indicate significant differences ($p < 0.05$).



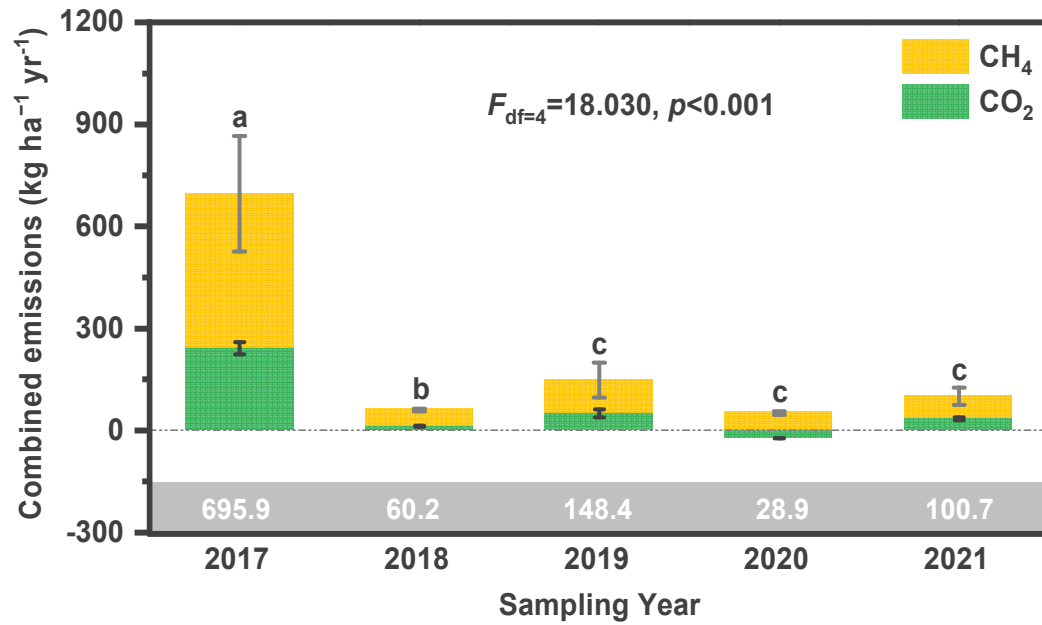
8

9

10

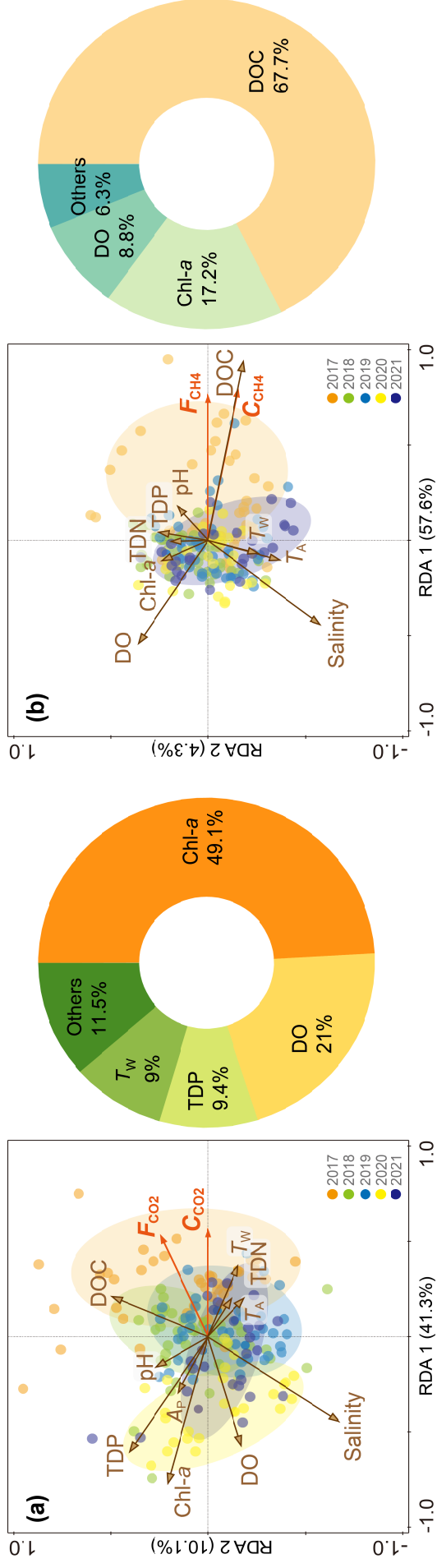
11

Figure 3 Box plots of dissolved GHG concentrations in surface water and diffusive GHG flux across water-air interface for coastal aquaculture ponds over a five-year period. Different letters above the boxes indicate significant differences ($p<0.05$; $n = 135$ for 2017, 225 for 2018, 126 for 2019, 81 for 2020, 81 for 2021).



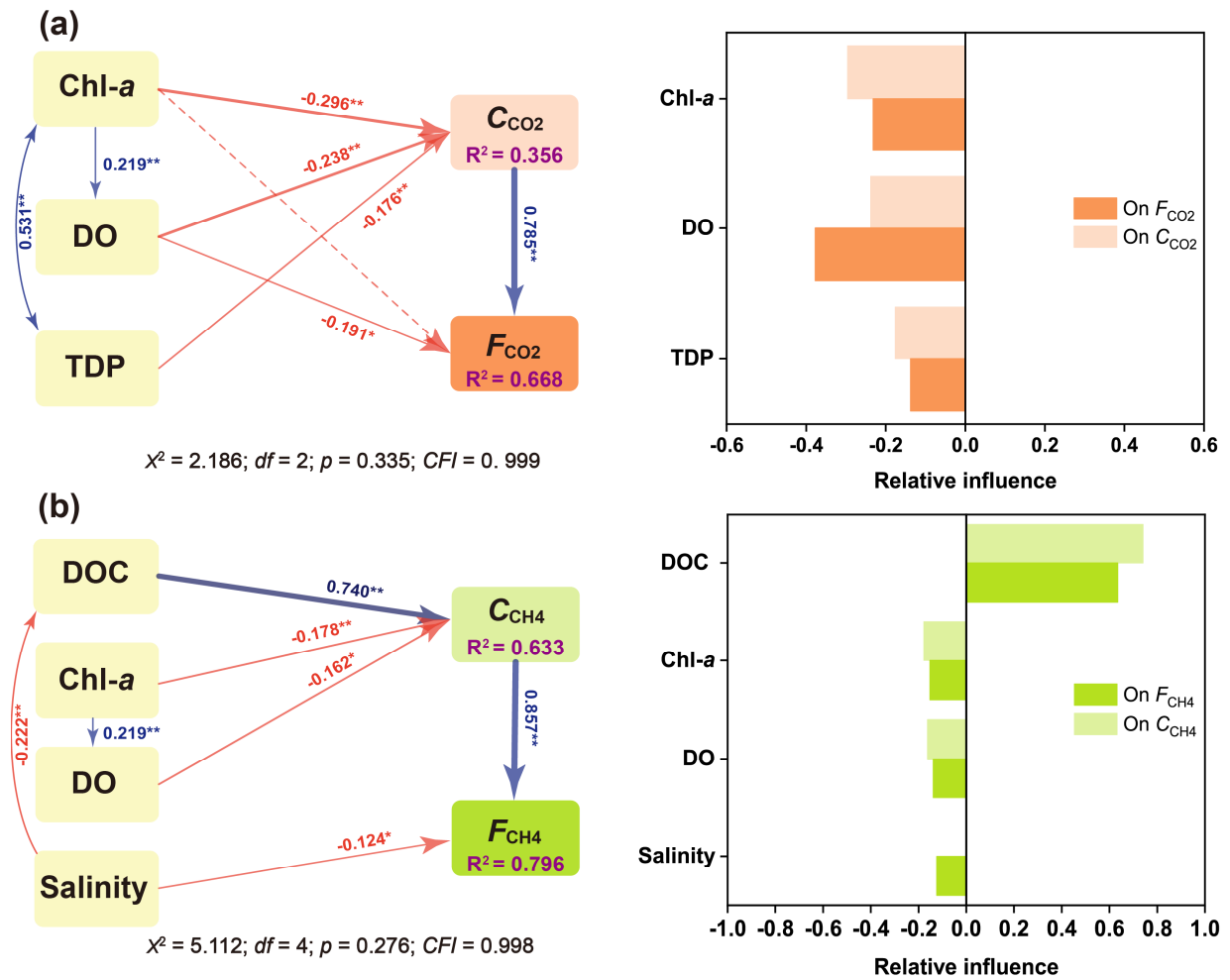
12

13 **Figure 4** Inter-annual variability in combined CO₂-equivalent emissions from the
 14 coastal aquaculture ponds during the farming period between 2017 and 2021.



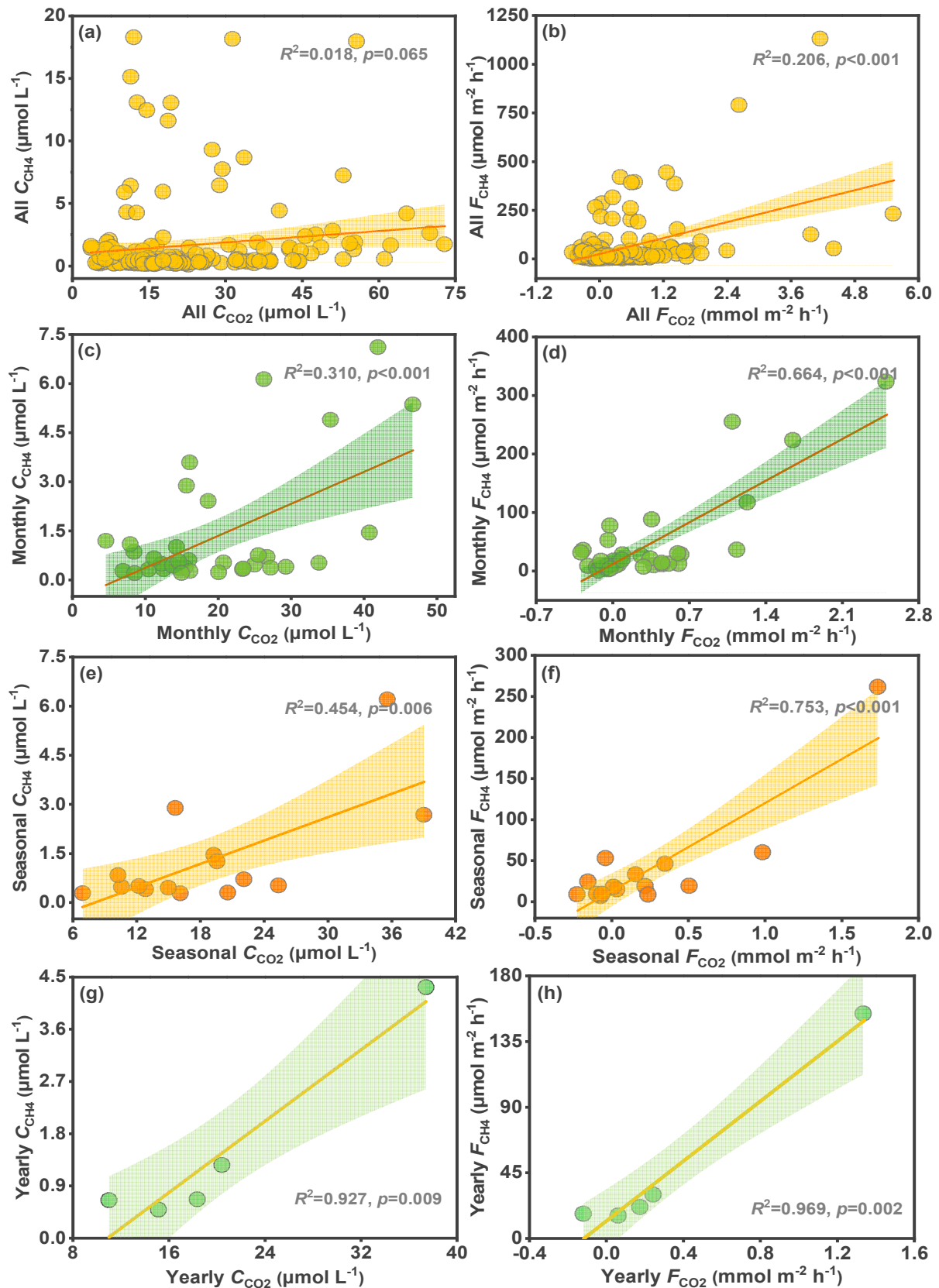
15

16 **Figure 5** Results of redundancy analysis (RDA) of (a) dissolved CO₂ concentration (C_{CO_2}) [or CO₂ diffusive fluxes (F_{CO_2}) across the water-air
 17 interface], and (b) dissolved CH₄ concentration (C_{CH_4}) [or CH₄ diffusive fluxes (F_{CH_4}) across the water-air interface], showing the loadings of the
 18 different environmental variables. The pie charts show the percentages of variance in CO₂ flux (or CO₂ concentration) and CH₄ flux (or CH₄
 19 concentration) explained by the different variables. See main text for explanation of the abbreviations.



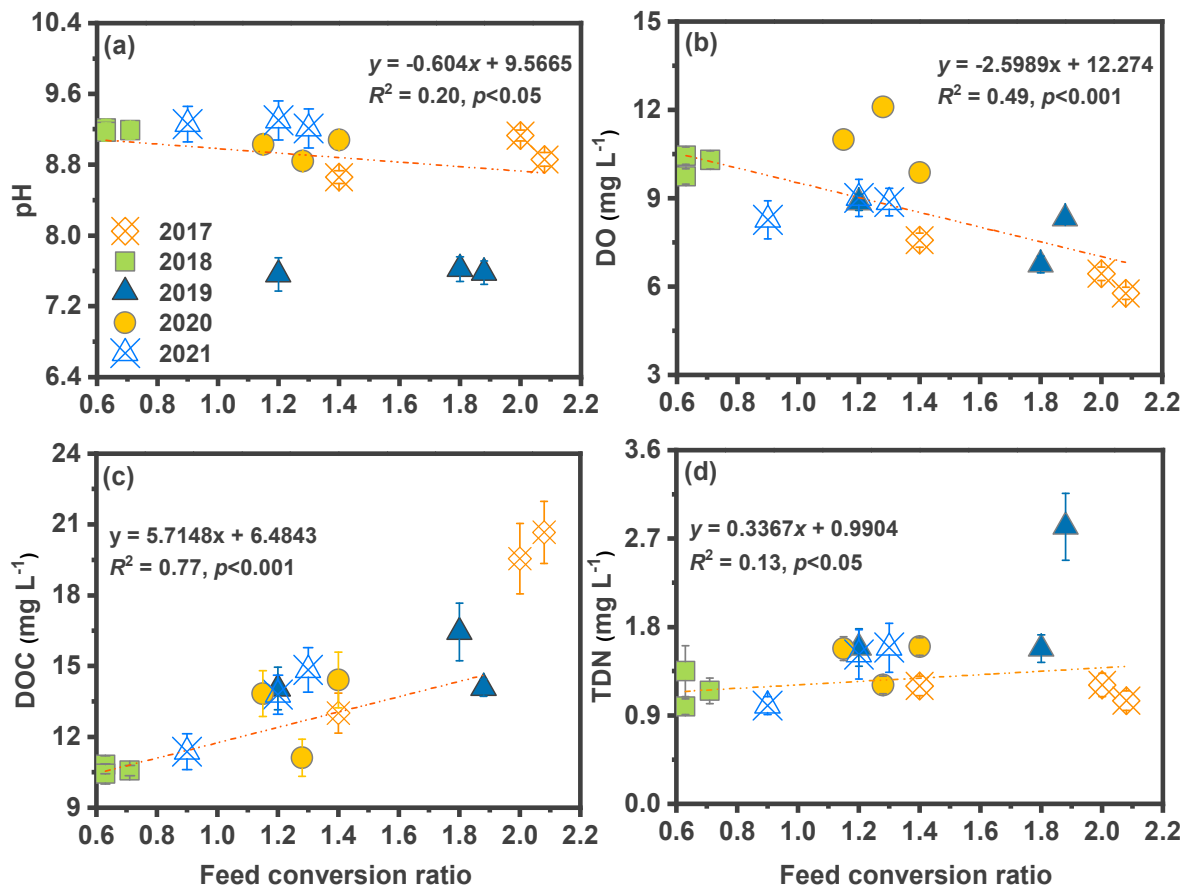
20

21 **Figure 6** Partial least square structural equation modeling (PLS-SEM) to evaluate the direct
 22 and indirect effects of environmental factors on (a) dissolved CO₂ concentration (C_{CO_2}) and
 23 CO₂ diffusive fluxes (F_{CO_2}) across the water-air interface, and (b) dissolved CH₄
 24 concentration (C_{CH_4}) and CH₄ diffusive fluxes (F_{CH_4}) across the water-air interface. Solid blue
 25 and red arrows indicate significant positive and negative effects, respectively, and dotted
 26 arrow indicates insignificant effect on the dependent variable. Numbers adjacent to arrows
 27 are standardized path coefficients, indicating the effect size of the relationship. R^2 represents
 28 the variance explained for target variables. * $p < 0.05$; ** $p < 0.01$.



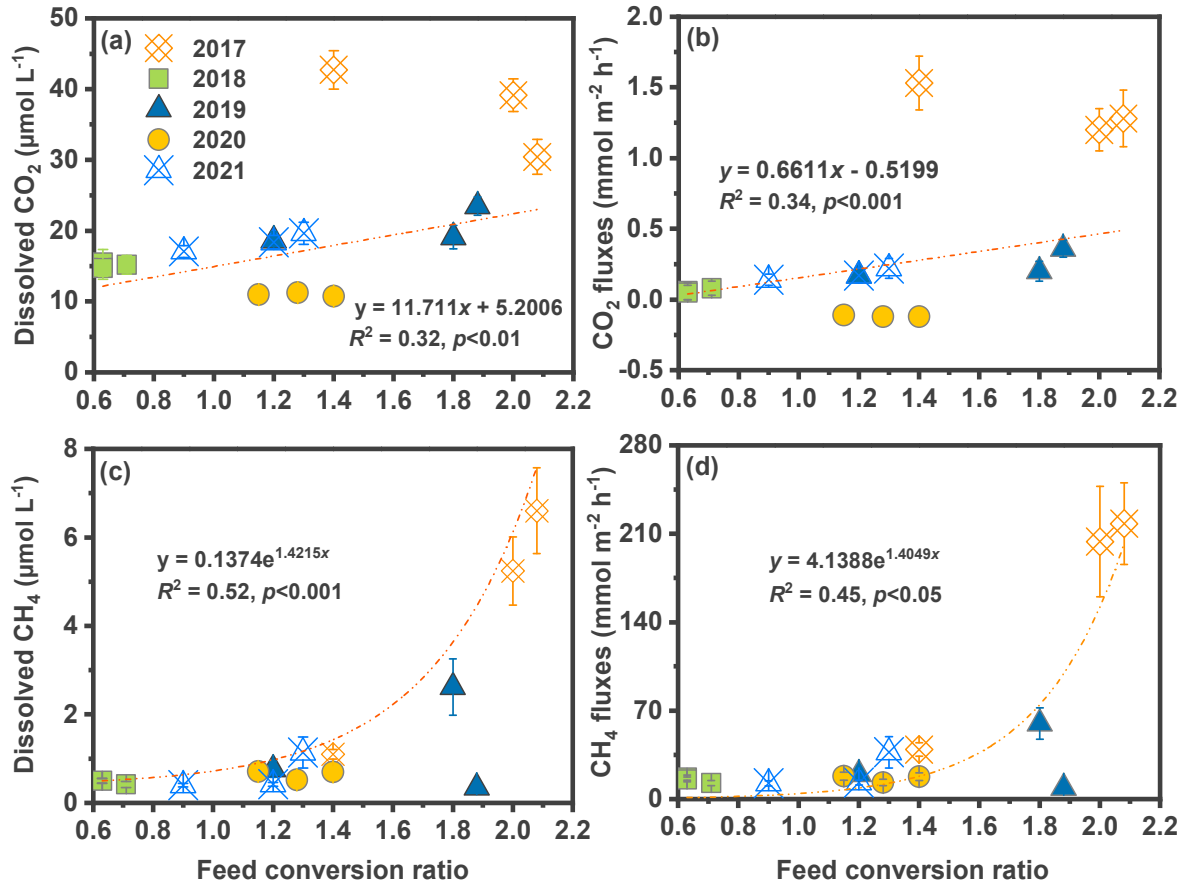
29

30 **Figure 7** Linear regressions between C_{CO_2} (or F_{CO_2}) and C_{CH_4} (or F_{CH_4}) using all data
 31 without binning, and data binned (averaged) by month, by season or by year. Output
 32 parameters of the regression analysis are listed in Table 1.



33

34 **Figure 8** Linear relationship between pH, DO, DOC, TDN and feed conversion rate
 35 (FCR) in coastal aquaculture ponds over a five-year period. Parameter bounds on the
 36 regression coefficients are 95% confidence limits. Feed conversion rate = dry weight of
 37 feeds added / wet weight of shrimps produced.



38

39 **Figure 9** Relationship between dissolved CO₂ concentration, diffusive CO₂ flux and feed
 40 conversion rate (a, b), and between dissolved CH₄ concentration, diffusive CH₄ flux and
 41 feed conversion rate (c, d) in coastal aquaculture ponds over a five-year period. Parameter
 42 bounds on the regression coefficients are 95% confidence limits.

Supporting Information

Significant inter-annual fluctuation in CO₂ and CH₄ diffusive fluxes from subtropical aquaculture ponds: Implications for climate change and carbon emission evaluations

Ping Yang^{a,b,c,d*}, Linhai Zhang^{a,b,c}, Yongxin Lin^{a,b,c}, Hong Yang^{e,f}, Derrick Y. F. Lai^g, Chuan Tong^{a,b,d*}, Yifei Zhang^a, Lishan Tan^e, Guanghui Zhao^a, Kam W. Tang^g

^a*School of Geographical Sciences, Fujian Normal University, Fuzhou 350007, P.R. China,*

^b*Key Laboratory of Humid Subtropical Eco-geographical Process of Ministry of Education, Fujian Normal University, Fuzhou 350007, P.R. China*

^c*Fujian Provincial Key Laboratory for Subtropical Resources and Environment, Fujian Normal University, Fuzhou 350117, P.R. China*

^d*Research Centre of Wetlands in Subtropical Region, Fujian Normal University, Fuzhou 350007, P.R. China*

^e*Department of Geography and Environmental Science, University of Reading, Reading, UK*

^f*College of Environmental Science and Engineering, Fujian Normal University, Fuzhou 350007, China*

^g*Department of Geography and Resource Management, The Chinese University of Hong Kong, Shatin, New Territories, Hong Kong SAR, China*

^h*Department of Biosciences, Swansea University, Swansea SA2 8PP, U. K.*

***Corresponding author:**

E-mail address: yangping528@sina.cn (P. Yang); tongch@fjnu.edu.cn (C. Tong)

Telephone: 086-0591-87445659 **Fax:** 086-0591-83465397

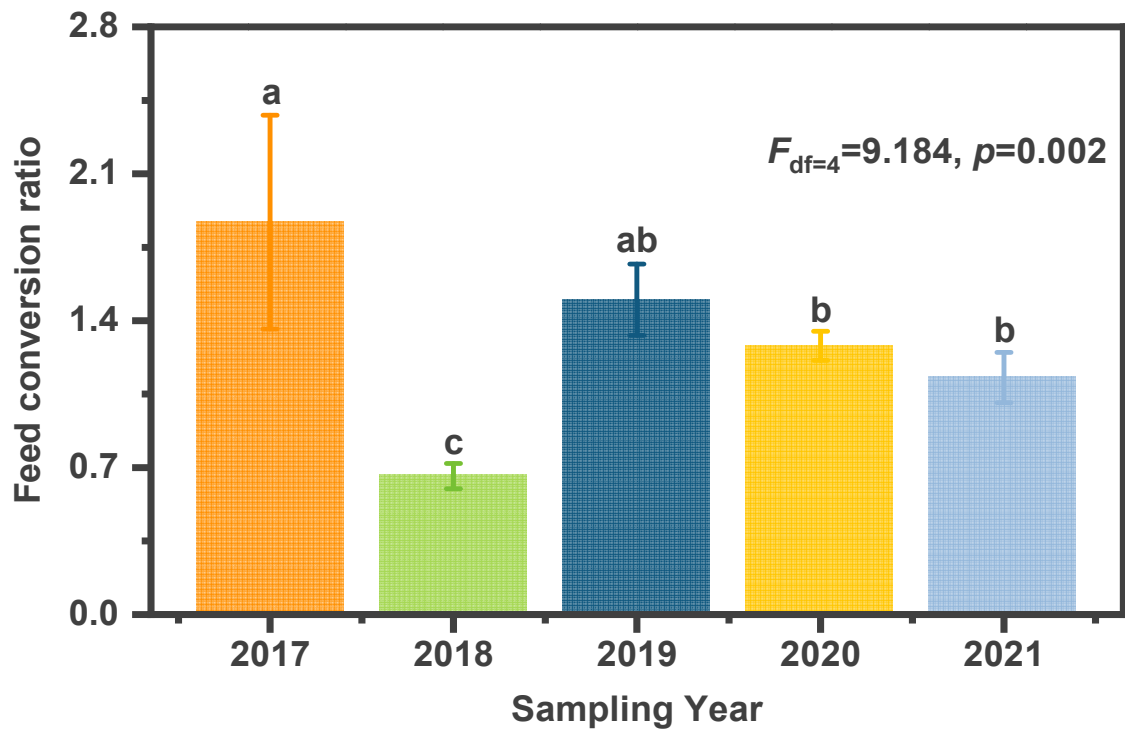
26 **Supporting Information Summary**

27 **No. of pages: 5 No. of figures: 3**

28 **Page S3:** Figure S1 Feed conversion ratio (FCR) of farmed organisms in the
29 aquaculture ponds during the farming period between 2017 and 2021.

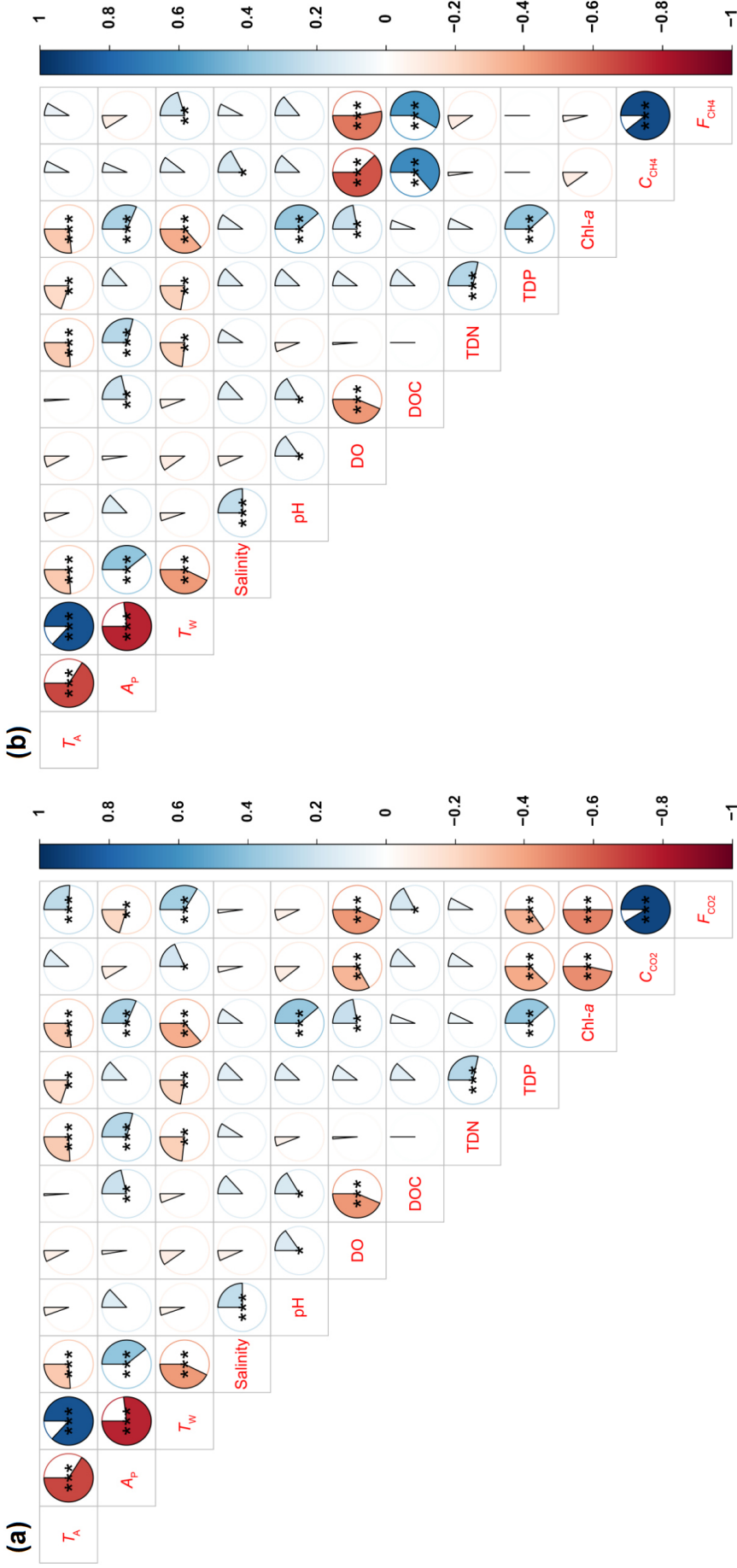
30 **Page S4:** Figure S2 Correlations among environmental variables and (a) dissolved CO₂
31 concentration (C_{CO_2}) and CO₂ diffusive fluxes (F_{CO_2}) across the water-air interface, and
32 (b) dissolved CH₄ concentration (C_{CH_4}) and CH₄ diffusive fluxes (F_{CH_4}) across the
33 water-air interface. Color of the pie indicates the direction of correlation (blue =
34 positive; red = negative). Size of the pie is proportional to the r^2 value. Asterisks
35 indicate levels of significance ($*p < 0.05$; $**p < 0.01$; $***p < 0.001$). See main text for
36 explanation of the abbreviations.

37 **Page S5:** Figure S3 Linear relationship between precipitation and salinity in coastal
38 aquaculture ponds over a five-year period. Parameter bounds on the regression
39 coefficients are 95% confidence limits.



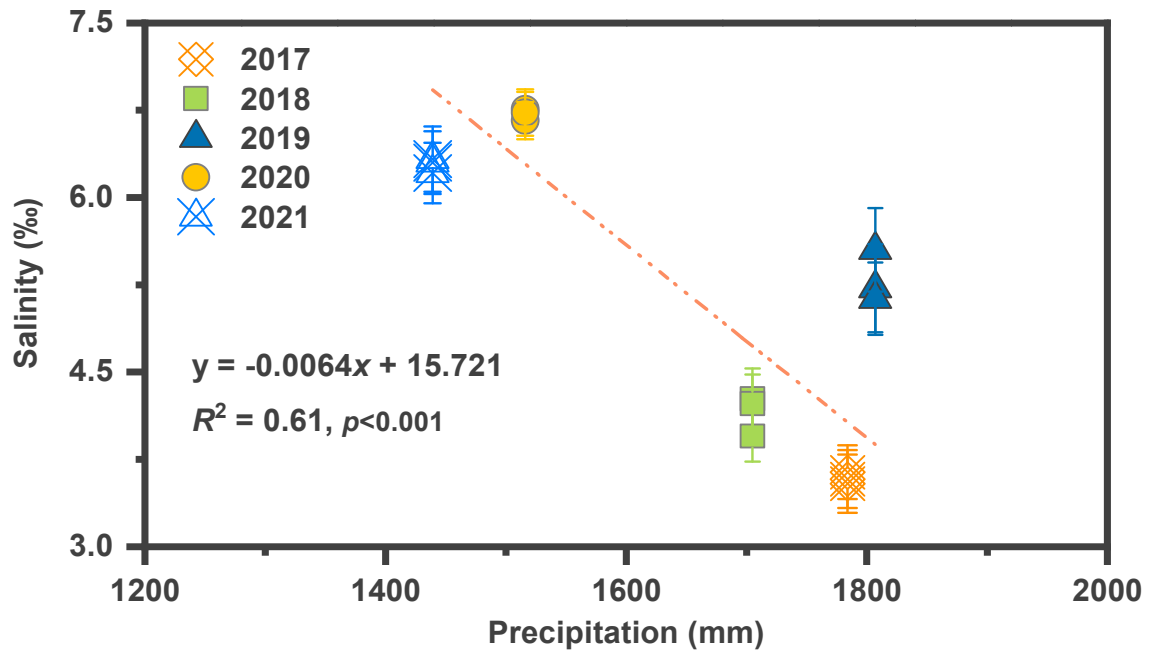
40

41 **Figure S1** Feed conversion ratio (FCR) of farmed organisms in the aquaculture ponds
42 during the farming period between 2017 and 2021.



43

44 **Figure S2** Correlations among environmental variables and (a) dissolved CO₂ concentration (C_{CO_2}) and CO₂ diffusive fluxes (F_{CO_2}) across the
 45 water-air interface, and (b) dissolved CH₄ concentration (C_{CH_4}) and CH₄ diffusive fluxes (F_{CH_4}) across the water-air interface. Color of the pie
 46 indicates the direction of correlation (blue = positive; red = negative). Size of the pie is proportional to the r^2 value. Asterisks indicate levels of
 47 significance ($*p < 0.05$; $**p < 0.01$; $***p < 0.001$). See main text for explanation of the abbreviations.



48

49 **Figure S3** Linear relationship between precipitation and salinity in coastal
 50 aquaculture ponds over a five-year period. Parameter bounds on the regression
 51 coefficients are 95% confidence limits.